X-Ray Diffraction – The Magic Wand

Iqra Zubair Awan*
Research Fellow, Institute Charles Gerhardt,
Ecole Nationale Superieure de Chimie, (34090) Montpellier, France.
Present: Faculty member, Dept. of Polymer Engineering and Technology,
University of the Punjab, Lahore, Pakistan
*iqrazubair@gmail.com

(Received on 6th September 2019, accepted in revised form 29th November 2019)

Summary: This review paper covers one of the most important discoveries of the last century, viz. X-ray diffraction. It has made enormous contribution to chemistry, physics, engineering, materials science, crystallography and above all medical sciences. The review covers the history of X-rays detection and production, its uses/ applications. The scientific and medical community will forever be indebted to Röntgen for this invaluable discovery and to those who perfected its application.

Keywords: Röntgen, X-rays, Braggs, Cathode Tube, Diffraction, Chemistry, Physics, Engineering, Medical and Health Sciences, Benefits, Hazards.

Introduction

X-rays were discovered in 1895 by Prof. Dr. Wilhelm Conrad Röntgen (1845 –1923). He had a German father and a Dutch mother. His early education was at a technical school in Utrecht (now a well-known university) but he was expelled for misbehavior. He then joined the Federal Polytechnic Institute, Zurich (now a famous university) from where he obtained a Ph.D in mechanical engineering in 1869. When his supervisor, Prof. Dr. August Kundt, moved to the University of Strasburg, he moved too. In 1874 Röntgen was appointed as a lecturer at the University of Strasburg; in 1875 he became Professor at the Academy of Agriculture, Hockenheim, Württemberg; in 1876 he became Professor of Physics and in Giessen and; in 1888 he became Professor of Physics at Würzburg and in 1900 at the University of Munich at the special request of the Bavarian government. He remained there till his death. [1]

Detection of X-rays – Historical Background

November 8th, 1895 is a historic day in the annals of science. The scientific and medical communities benefitted most from his discovery. All through 1895, Röntgen investigated the effects of an electric discharge passing through various types of vacuum tube equipment from Heinrich Herz, Johann Hittorp, William Crookes, Nikola Tesla and Phillip von Lenard [1-5]. At the beginning of November of that year he repeated an experiment with one of Lenard's tubes. He had added a thin aluminium window to allow the "cathode rays" to pass through the tube. A cardboard cover was also added to shield the aluminium from damage of the strong electrostatic field that produces the cathode rays (a brief description of this is given at the end of this section). He knew that the cardboard covering would prevent light from escaping. Non-the-less he observed that the invisible cathode rays caused a fluorescent effect on a small cardboard screen placed on a table 6 feet away. The screen had been painted with barium platinocyanide crystals and it glowed when he activated the tube. Even after covering the tube with black cardboard, it still kept glowing. Röntgen named this strange phenomenon X-rays (X being any unknown factor in scientific jargon). In follow-up experiments, he used a photographic plate and made the first ever X-ray pictures, one of them of the now famous hand of his wife, Anna Bertha (Fig. 1). From 1879 on, many scientists, including Sir William Crookes, were interested in the newly discovered cathode rays (Radiant Rays) (Fig. 2). X-rays and Röntgen soon became very familiar names in the scientific world.

Fig. 1: The first radiographic observation of the hand of Röntgen's wife, Bertha. [1].

*To whom all correspondence should be addressed.

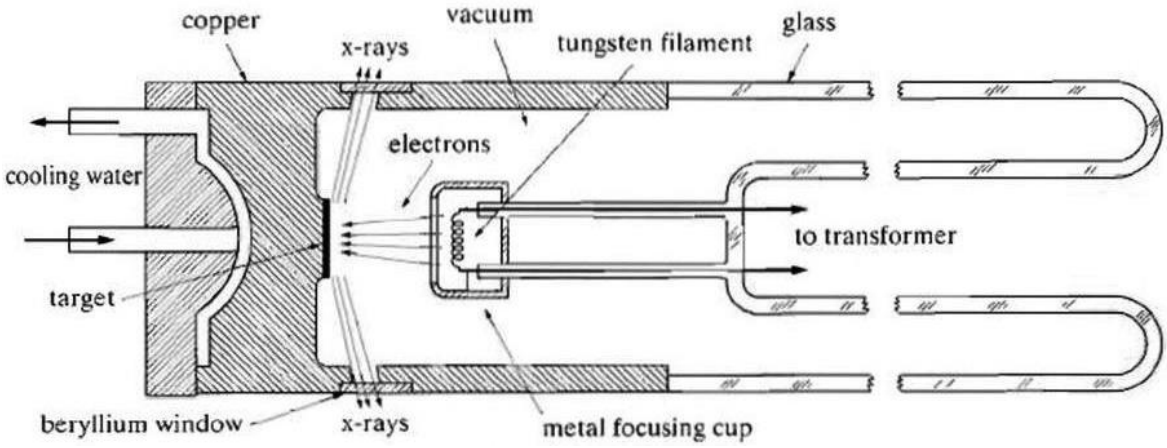

Fig. 2: Cross section of a sealed x-ray cathode tube (schematic). [2]

Since cathode tubes/rays played a very important role in the discovery of X-rays, a brief description of this important instrument/rays is given below.

Cathode Ray Tubes and Cathode Rays

Cathode Tubes

After many decades of efforts and investigations, the basic structure of matter was solved with the help of experiments that started with the study of discharges in evacuated tubes in the late 19th century. Similarly a number of discoveries were made which were responsible for the technological revolution of the 20th century.

William Crookes' (1832-1919) investigated electric discharges in gases, followed by the invention of the cathode ray tube (Fig. 2) and his studies on cathode rays and the dark space at the cathode, led to the discovery of X-rays and of the electron. In 1897 Crookes was knighted by Queen Victoria and in 1909 he was elected President of the Royal Society.

Cathode Rays

Cathode rays are considered to be energetic electrons traveling from the cathode to the anode. They are generated in a cathode ray tube, (Fig. 2). The electrons are generated at the cathode by thermionic emission and are attracted towards the screen by the anode, which is further connected to the terminal of the extra high-tension battery (E.H.T.). During thermionic emission process the metal surfaces emit electrons when heated. A vacuum is created in the tube in order to avoid interaction of electrons with any particle before they reach the screen. As soon as the cathode rays hit the fluorescent screen, the screen glows. This reveals that electrons possess momentum and, therefore, have mass.

Properties of Cathode rays

It was Joseph Thomson (1856-1940) who provided excellent evidences that cathode rays composed of charged particles. He calculated mass to charge ratio and comprehensively estimated that the mass was equal to 1/1800 of the mass of a hydrogen atom. He won the Noble Prize in 1906 for the discovery of the electron.

Cathode rays are negatively charged and move in straight lines. They can be deflected by magnetic and electric fields, proving that they are charged particles. They induce fluorescence in certain materials. When they are hindered by heavy metals, they produce X-rays. They are electrons moving at high speed. If an opaque object is introduced in the path of the cathode rays, a sharp shadow of the object is cast on the fluorescent screen.

X-rays – Generation and Properties

X-rays are short wave-length radiations (photons) with a wave length to the order of 10 Ångstrom to 0.01 Ångstrom. They are highly penetrating but can be observed in dense matter such as lead and tungsten (used for protective shielding). Upon being absorbed, they transfer all or part of their energy to electrons in the material, thereby ionizing the material [6].

X-rays can be produced in two ways. The first process is called Bremstralung (from German meaning "braking radiation") (Fig. 3). As an electron at A moves at high speed in the immediate vicinity of a heavy nucleus (i.e. impacting on a solid metal target) it has rapid negative acceleration, loses energy and, in terms of the wave theory, radiation is emitted. In quantum terms, the

energy emitted is in the form of photons (short wave-length radiation) each having a definite frequency. The negative acceleration (braking) of the electron can occur either as a result of its actually being stopped (braked) by collision with the nuclei of the target material, or merely by having its direction changed, velocity being a vector quantity (Fig. 3).

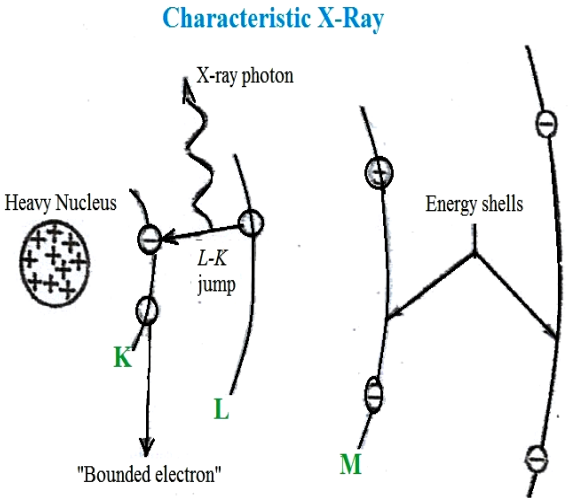

Fig. 3a: Schematic diagram of the production of characteristic x-rays. Only those electrons "jumps" that occur in the innermost shells or orbits involve enough energy to produce x-ray photons. [6]

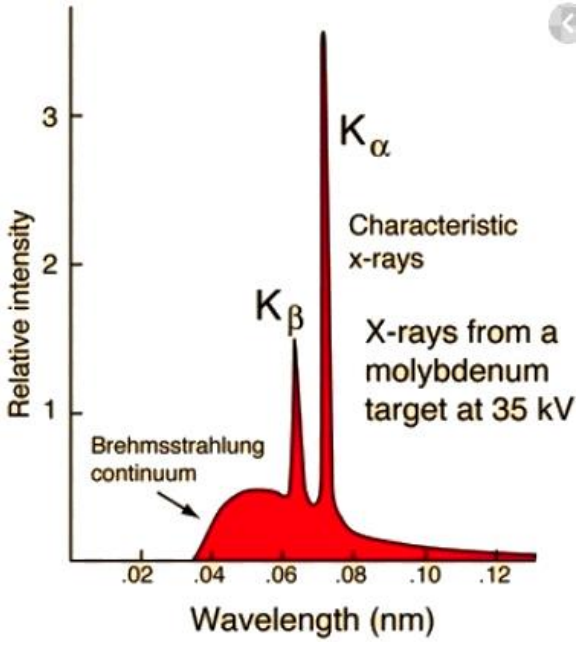

Fig. 3b: Characteristic x-rays. [6].

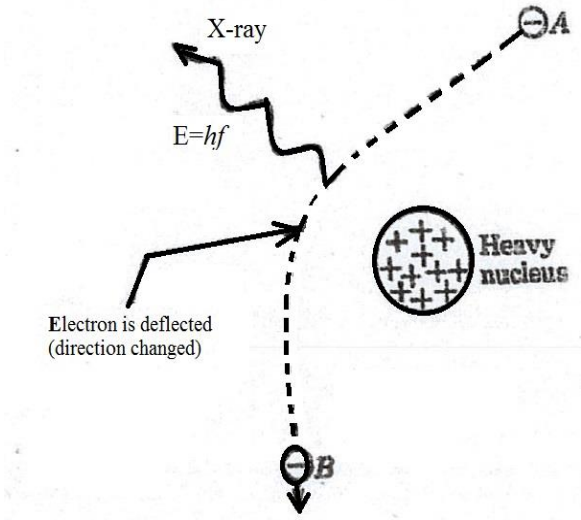

Fig. 3c: Schematic diagram illustrating braking radiation (*bremsstrahlung*). [6].

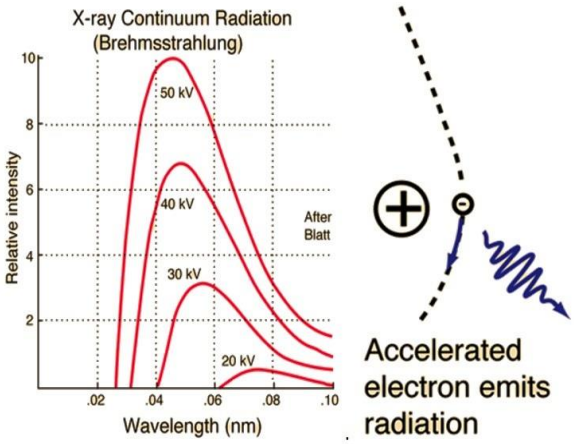

Fig. 3d: Bremsstrahlung x-rays. [6]

The target in an X-ray tube (Fig. 4) must be a metal with heavy nuclei, atomic numbers of $Z \geq 40$ being typical for X-ray production. A great deal of heat is generated in the collision (or braking) process, so materials with high melting points must be used. Tungsten is commonly used as target material. Provision for cooling the tube is usually made. When the cathode rays (electrons) collide with the target, 99% of the kinetic energy of the electrons turns into heat energy while 1% is converted into X-rays. The heat produced at the target is cooled with the help of copper cooling fins mounted on the copper anode. Heat is conducted away from the tube by conduction and radiation. The electron current, I in an X-ray tube in operation is given by I = ne, where n is the number and e is the electron charge.

.

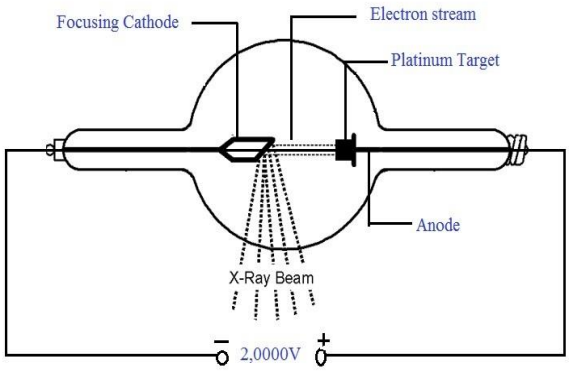

Fig. 4: (a) Diagram of an early x-ray tube.

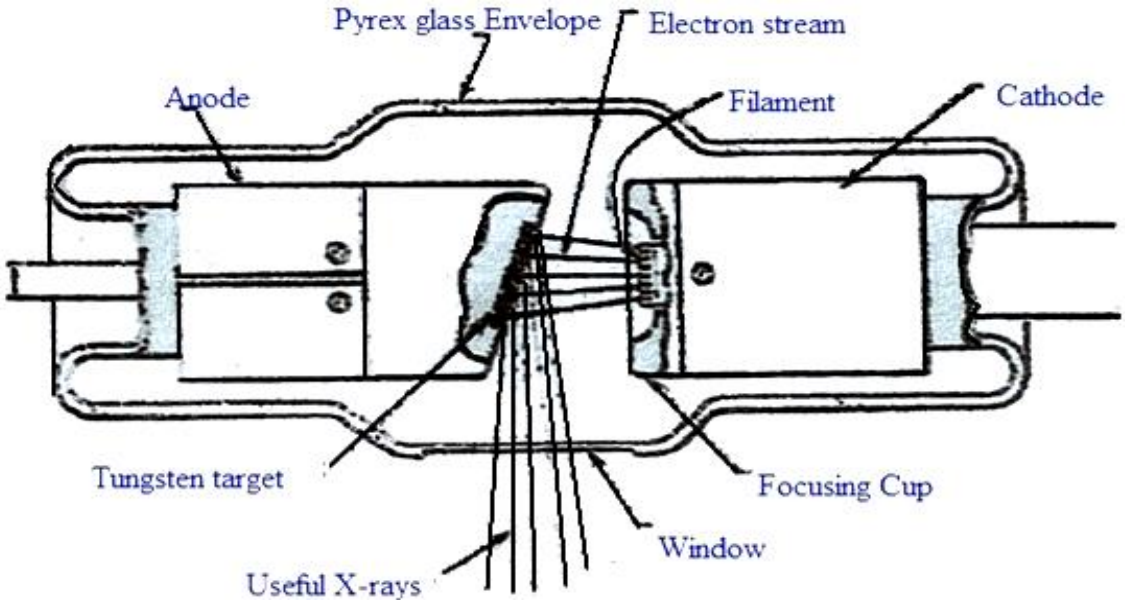

Fig. 4: (b) Diagram of Coolidge x-ray tube with parts labeled. [6].

For the emission of a single photon, as an electron is "braked" from velocity *v* to velocity *v'*, the conservation-of-energy equation is

$$E = hf = \frac{1}{2}mv^2 - \frac{1}{2}mv'^2 \quad (1)$$

The maximum photon frequency is produced when an electron is completely stopped and *v'* becomes zero. In that case the frequency can be found from

$$E = hf_{max} = \frac{1}{2}mv^2 \quad (\textit{the x-ray equation}) \quad (2)$$

In order to provide electrons of high kinetic energy, they are accelerated in the X-ray tube by a high potential difference, ordinarily of 10 kV or more. The electron potential energy-to-photon kinetic energy conversion can be expressed as

$$Ve = KE = \frac{1}{2}mv^2 \quad (3)$$

$$Ve = \frac{1}{2}mv^2 \quad (4)$$

Combining equations (2) and (3) and using $f = c/\lambda$, we obtain

$$Ve = h\frac{c}{\lambda} \text{ from which } \lambda = \frac{hc}{Ve} \qquad (5)$$

Substituting known physical constants, the *minimum* X-ray wavelength is given by

$$\lambda_{min} = \frac{\left(6.626\,\mathbf{x}\,10^{-34}\ \text{J-sec}\right)\left(3\,\mathbf{x}\frac{10^{8}\,\text{m}}{\text{sec}}\right)}{(1.602\ \mathbf{x}\ 10^{-19}\ \text{C})\mathbf{x}\ \text{V}}$$

Since coulombs = joules/volts, or C = J/V, and 1 Å = 10^{-10} m, it follows that

$$\lambda_{min} = \frac{12400\ \text{volts}}{V}\ \text{Å} \qquad (6)$$

Equation (5) says that an applied voltage *V* of 12,400 volts produces X-ray photons with a minimum wavelength of 1 Å of the X-rays from an X-ray tube, divide 12,400 volts by the voltage applied across the tube. Typical accelerating voltages range from 10 kV up to 2 MV or more.

Braking-radiation X-ray production is often referred to as the inverse photoelectric effect. In the photoelectric effect, photon energy is converted to photoelectron energy. In X-ray production, electron energy is converted to the energy of X-ray photons. The basic equation for X-ray production, $hf_{max} = \frac{1}{2}mv^2$, is just the photoelectric equation, $hf = \frac{1}{2}mv^2 + \phi$, with the work function ϕ = zero.

Characteristic X-rays

The second mechanism for creating X-rays involves electron transitions between energy levels, as an electron "move" from one orbit to another of an atom. In heavy atoms (i.e. with heavy nuclei), *energy shells* have been identified and labeled *K, L, M, N,* etc. When a high-speed electron collides with a tightly bound electron in the innermost (*K*) shell, it may transfer enough energy to knock that electron out of the atom. A vacancy is thus created, and an electron from a higher-energy shell may move in to fill the vacancy, thereby creating a new vacancy (Fig. 5). Other electrons change shell locations until the vacancy moves to the outside of the atom. A number of photons are emitted.

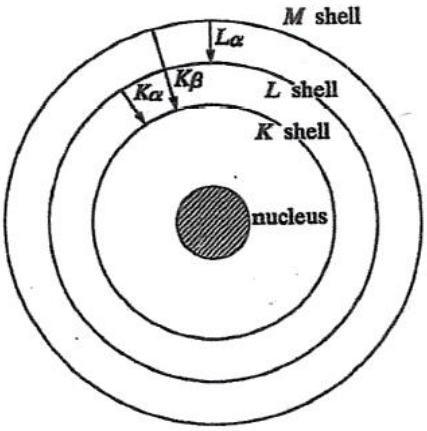

Fig. 5: (a) Electronic transitions in an atom (schematic). Emisson processes indicated by arrows. [6]

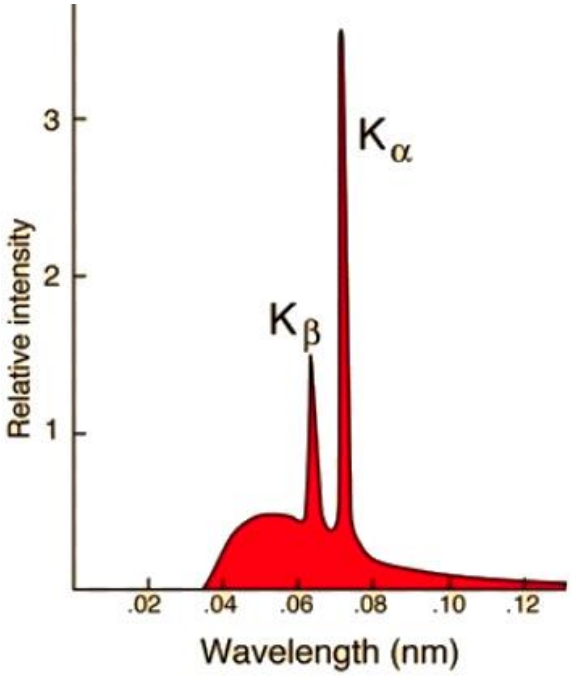

Fig. 5: (b) Emission spectrum of a molybdenum anode bombarded with an electron beam. [6].

The Compton Effect

Arthur H. Compton (1892-1962) was investigating the properties of X-rays in 1922. He found that when a beam of X-rays strikes a target of solid carbon, the X-rays are "scattered" and their wavelength is slightly increased. Classical wave theory would predict that when an electron is "struck" by an electromagnetic wave, the electron would oscillate with the same frequency as the (X-ray) wave,

and would radiate energy of that same frequency (wavelength).

Since classical wave theory could not account for the increased wavelength, Compton turned to the photon idea. He assumed that the X-rays used in the bombardment were X-ray photons (i.e. particle-like rather than wave-like). Each photon is assumed to possess kinetic energy and momentum, and to have the capability of having elastic collisions with other particles of matter. In Fig. (6), suppose *hf* is an X-ray photon approaching collision with a free electron $\bar{e}$, in a carbon block. This incident photons transfers some of their energy to the electron, which is accelerated and moves off in the direction shown. The energy gained by the electron from incident X-ray photon shows up in a change of velocity (and also direction, since velocity is a vector quantity). In the diagram, the "scattered" X-ray photon is shown moving upward and to the right. For the photon, since $E - hf$ is less than it was before the collision, and since *h* is a constant, *f* must decrease to some value *f ′*. A decreased frequency means an increased wavelength, which is precisely the experimental finding. The Compton effect, then, is one more in a series of twentieth-century experimental findings that support the quantum idea and the photon theory of light.

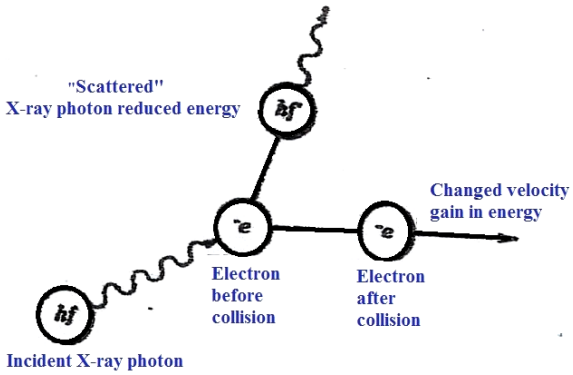

Fig. 6: Diagram illustrating the Compton effect. [6]

Wave-Particle Duality

Einstein's explanation of the photoelectric effect shows that light does not always behave as if it were a wave. In forcing the emission of electrons from a metal, light acts like a particle with a quantized energy, $E = hf$. Einstein's "model" is supported by actual laboratory observations and confirms the predicted relationship between energy, frequency, and the constant *h* (Planck's constant).

For X-rays, the quantum-theory model also calls for the equation $E = hf = \frac{1}{2}mv^2 = Ve$. Careful laboratory investigations again confirm the particle or photon theory and likewise with the Compton effect. But equally competent experiments and theorists had earlier developed the wave theory of light, and the entire science of optics is based on light as a wave motion. Electromagnetic wave theory is also the basis for radio, television, radar, and microwave devices. Since these devices – optical equipment and communications equipment – are conceived, designed, manufactured, and successfully operated on a wave-theory model, it is unlikely that the wave theory is wrong.

It would appear, therefore, that there are two mutually incompatible theories on the nature of light and electromagnetic radiations. And, rather than ask which theory is right and which is wrong, we are forced by circumstances to admit that they are probably both right. It seems that light is both wave-like and particle-like, with irrefutable evidence supporting both views. However, wave characteristics and particle characteristics do not seem to occur simultaneously or in the same process. For example, a beam of light can be refracted and undergo dispersion (color separation) through optical equipment, obeying well-known wave-theory patterns of behavior, and immediately thereafter shine on a photocell and act like a stream of photons, but they never occur at the same time. Two generalizations are possible: (1) Concerning the propagation of light (and electromagnetic radiation in general), the wave theory seems to be obeyed. (2) When light (or electromagnetic radiation) strikes or interacts with atoms, molecules, electrons, neutrons, or other subatomic units, it acts like particles or photons.

In summary, the two theories complement each other; both are "correct" under certain circumstances. Neither gives us a "picture" of the true nature of light, but both help us understand the behavior of light and electromagnetic radiations. Pending further discoveries which might provide a basis for a single unifying theory, it seems that we must accept both the wave theory and the photon (quantum) theory of light.

The intensity of the X-rays in a tube is proportionate to the number of electrons hitting the target. The filament supply determines the number of electrons generated at the cathode. The more intense is the heating current, the larger the number of electrons is generated will be and thus more X-rays are produced. It is now established that the intensity of X-

rays is controlled by the filament current. The penetration power of the X-rays is directly proportional to the kinetic energy of the electrons colliding with the target. The more intense is accelerating voltage, the faster the electrons will be produced. Faster electrons have higher kinetic energy and produce X-rays of shorter wavelength and greater penetration power. Thus the penetrating power of X-rays is established by the accelerating voltage across the tube. There are two kinds of X-rays (hard and soft). Hard X-rays have a high penetrating power due to very short wavelengths. They are generated when a high p.d is applied through the tube. Soft X-rays are formed by the electrons traveling at lower velocities compared those produced by hard X-rays. Less energy and longer wavelengths give them less penetration power than hard X-rays. Hard X-rays pass through flesh but are absorbed by bones. Soft X-rays reveal malignant growths and are readily absorbed by such growths.

To recapitulate, X-rays move in straight lines at the speed of light and are not deflected by magnetic or electric fields. This indicates that they bear no charge. They are capable of penetrating in all matter to some extent. The penetration of these rays is lower in materials with high density and atomic number e.g. lead. They ionize gases which received these rays. They affect photographic plates in the same way as light does. They induce fluorescence in some materials. They are also responsible for photoelectric effect when illuminated onto certain metal surfaces. The X-rays are also diffracted by crystals hence leading to an interference pattern. X-rays are used for (1) Stresses, fractures in solids structural analysis, , castings and welded joints can be analyzed by examining X-ray photographs. (2) Crystallography; identification and orientation of minerals by analysis of diffraction patterns using Bragg's law. (3) Medical uses; (i) Analytical uses: These include identification of fractures, location of cancers and tumors. Sick tissue absorbs X-rays differently from normal tissue. (ii) Therapeutics use for destroying cancerous cells and tumors.

We will first explain the various diffraction methods and applications thereof, and then the various equipment used for such applications.

Diffraction methods

We will first discuss the diffraction methods used for materials characterization (i.e. application to materials analysis) and then for medical purposes.

Diffraction methods for materials characterization

Since crystals have symmetrical arrays of atoms bearing rows and planes of high atomic density, capable to act as three-dimensional diffraction gratings. If light rays are to be properly diffracted by a grating, then the spacing of the grating (distance between ruled lines on a grating) must be more or less equal to the wavelength of the light waves. In the case of visible light, gratings with line separations between 10,000 and 20,000 Å units are used to diffract wavelength in the range from 4000 to 8000 Å. In crystals, however, the separation between equally parallel rows of atoms or atomic planes is much smaller – to the order of a few Å units. Fortunately, low-voltage X-rays have wavelengths of the proper magnitudes to be diffracted by crystals; that is, X-rays produced by tubes operated in the range between 20,000 and 50,000 volts, as contrasted to those used in medical applications, where voltage exceed 100,000 volts.

When X-rays of a specific frequency collide an atom and subsequently interacting with its electrons, causing them to vibrate with the frequency of the X-ray beam. Since these electrons are now vibrating electrical charges, they reradiate the X-rays with no change in frequency. These reflected rays shoot off the atoms in any direction. In other words, the electrons of an atom "scatter" the X-ray beam in all directions [7].

When atoms spaced at regular intervals are irradiated by a beam of X-rays, the scattered radiation undergoes interference. In certain directions constructive interference occurs; in other directions destructive interference occurs. For instance, if a single atomic plane is struck by a parallel beam of X-rays, the beam undergoes constructive interference when the angle of incidence equals the angle of reflection. Thus, in Fig. (7), the rays marked a_1 to a_3 represent a parallel beam of X-rays. A wave front of this beam, where all rays are in phase, is shown by the line *AA*. The line *BB* lies at the same distance from the wave front *AA* when measured along any ray, all points on *BB* must be in phase. It is, therefore, a wave front, and the direction of the reflected rays is a direction of constructive interference." [7].

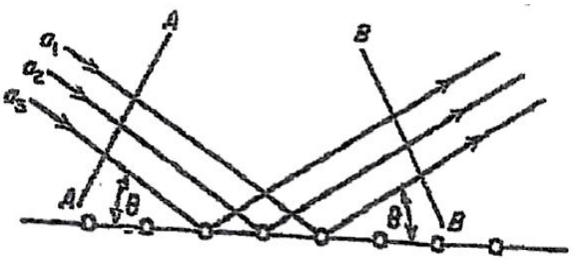

Fig. 7: An x-ray beam is reflected with constructive interference when the angle of incidence equals the angle of reflection. [7].

The Bragg Law

The above discussion does not depend on the frequency of the radiation. However, when the X-rays are reflected, not from an array of atoms arranged in a solitary plane, but from atoms on a number of equally spaced parallel planes, such as exist in crystals, then constructive interference can occur only under highly restricted conditions. This is known as Bragg's Law. For a closer examination, let us consider each plane of atoms in a crystal as a semitransparent mirror, i.e. each plane reflects a part of the X-ray beam and also permits part of it to pass through. When X-rays strike a crystal, the beam is reflected from both the surface layer of atoms as well as from atoms underneath the surface to a considerable depth. Fig. (8) shows an X-ray beam that is being reflected simultaneously from two parallel lattice planes. In a real case, the beam would be reflected, not only from two lattice planes, but from a large number of parallel planes. The lattice spacing, or distance between planes, is represented by the symbol d in Fig. (8). The line oA_i is drawn perpendicular to the incident rays and is therefore a wave front. Points o and m, which lie on this wave front, must be in phase. The oA_r is drawn perpendicular to the reflected rays a_1 and a_2, and the condition for oA_r to be a wave front is that the reflected rays must be in phase at points o and n. [7].

Let us assume that the X-ray beam has a minimum wavelength of 0.5 Å, that it makes a 60° angle with the surface of the crystal which, in turn, is assumed to be parallel to a set of {100} planes. Also, that the {100} planes have a spacing of 1 Å. Substituting these values in the Bragg equation gives

$$n\lambda = 2d \sin \theta \qquad (7)$$

or

$$n\lambda = 2(1) \sin 60^{o} = 1.732 \qquad (8)$$

Thus, the rays reflected from {100} planes will contain the wavelengths

1.732 Å	for first-order reflection
0.866 Å	for second-order reflection
0.546 Å	for third-order reflection

All other wavelengths will suffer destructive interference.

In these examples, the reflecting planes were assumed to be parallel to the crystal surface. This is not a necessary requirement for reflection; it is quite possible to obtain reflections from planes that make all angles with the surface. Thus in Fig. (9), the incident beam is shown normal to the surface and a (001) plane, while making an angle θ with two {210} planes – (012) and (0$\bar{1}$2). The reflections from these two planes are shown schematically in Fig. (9). This leads to the conclusion that, when a beam of white X-rays collides a crystal, many reflected beams will emerge from the crystal. Each reflected beam will correspond to a reflection from a different crystallographic plane. Furthermore, in contrast to the incident beam that is continuous in wave length, each reflected beam will bear only discrete wavelengths as prescribed by the Bragg equation [7].

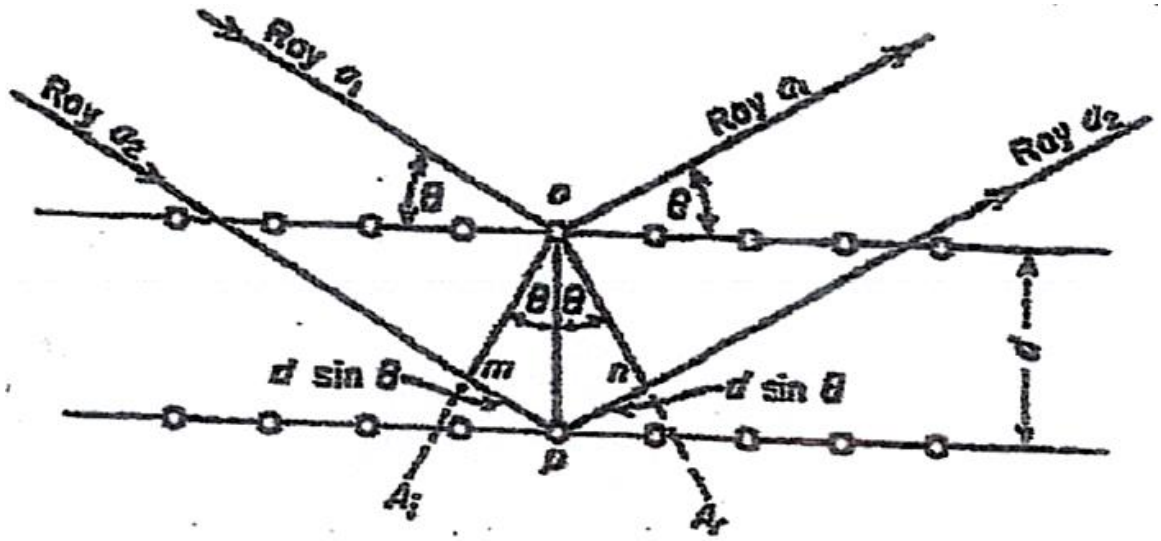

Fig. 8: The Bragg Law. [7]

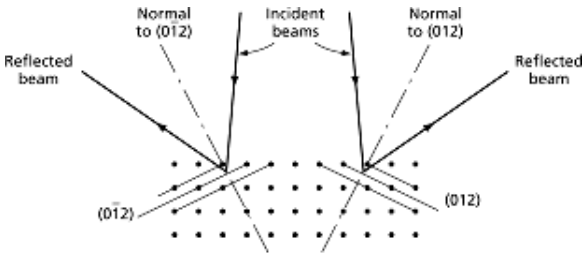

Fig. 9: X-ray reflections from planes not parallel to the surface of the sample. [7].

Laue Techniques

The Laue X-ray diffraction methods use a crystal with an orientation that is fixed with respect to a beam of continuous X-rays, as described in the preceding section. There are two basic Laue techniques; in one, the beams reflected back in directions close to that of the incident X-ray beam are studied – the back-reflection Laue technique. In the other, the reflected beams that pass through the crystal are studied – the transmission Laue technique. The latter method cannot be applied to crystals with a thickness of 1 mm or more because of the loss in intensity of the X-rays through being absorbed by the metal.

The back-reflection Laue method is especially useful for determining the orientation of the lattice inside crystals when the crystals are large and therefore opaque to X-rays. Many physical and mechanical properties vary with direction inside crystals. These anisotropic properties of crystals require knowledge of the lattice orientation in the crystals. [7]

Fig. (10) gives the set-up of a typical Laue back-reflection camera. X-rays from the target of an X-ray tube are collimated into a narrow beam by a tube which has an internal diameter of about 1mm and is several inches long. This narrow beam of X-rays strikes the crystal on the right of the figure. Here it is diffracted into a number of reflected beams that strike the cassette containing a photographic film. The front of the cassette is covered with a thin sheet of material like black paper. Light cannot pass through this barrier but reflected X-ray beams can. The positions of the reflected beams can now be recorded on photographic film and appear as a pattern of small dark spots. [7]

In Fig. (11), the back-reflection X-ray pattern of a magnesium crystal, oriented so that the incident X-ray beam was perpendicular to the basal plane of the crystal, is shown. The reflection of each single crystallographic plane corresponds to a spot and the six-fold symmetry of the lattice, when viewed in a direction perpendicular to the basal plane, is obvious. When the crystal is rotated away from the orientation of Fig. (11), the pattern of spots changes (Fig. 13). However, it still defines the orientation of the lattice in space. The orientation of a crystal can thus be determined in terms of a Laue photograph." [7].

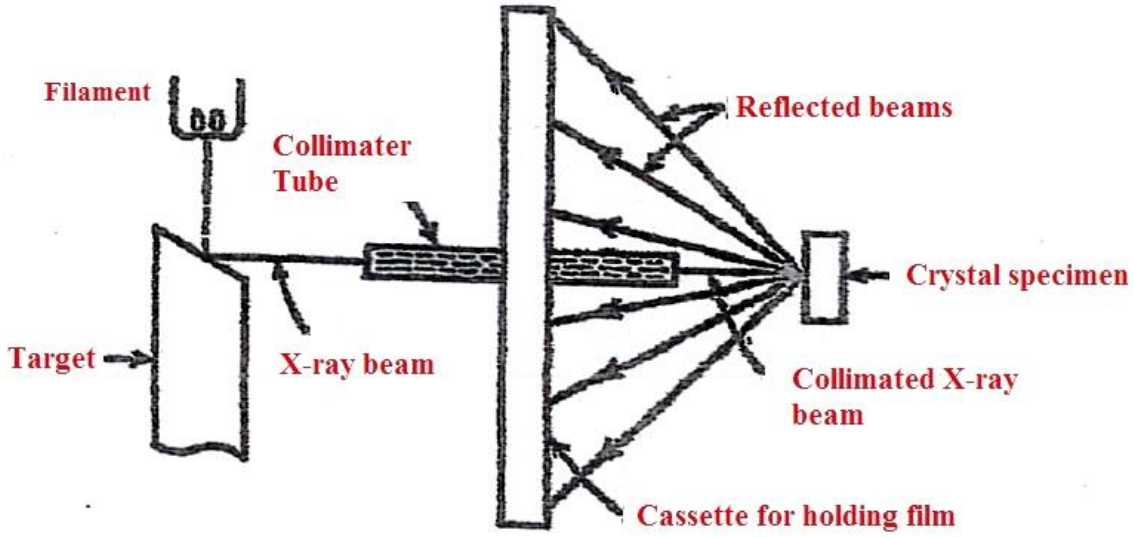

Fig. 10: Laue back-reflection camera. [7].

Fig. 11: Laue back-reflection photographs:
(A) with x-ray beam perpendicular to the basal plane (0001);
(B) with x-ray beam perpendicular to a prism plane (1120).
Dashed lines on the photograph are drawn to show that the back-reflection spots lie on hyperbolas. [7]

Transmission Laue patterns can be obtained with an experimental arrangement similar to that for back-reflection patterns, but the film is placed on the opposite side of the specimen from the X-ray tube. Specimens may be shaped as small rods or plates, but the dimension parallel to the X-ray beam should be small. The back-reflection technique reflects the X-ray beam from planes nearly perpendicular to the beam itself. The transmission technique records the reflections from planes nearly parallel to the beam. (Fig.12)." [7]

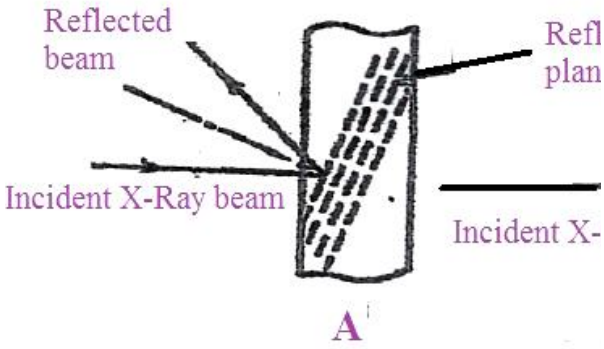

Fig. 12: (A) Laue back-reflection photographs record the reflections from planes nearly perpendicular to the incident x-ray beam.
(B) Laue transmission photographs record the reflections from planes nearly parallel to the incident x-ray beam. [7].

Fig. 13: Asterism in a Laue back-reflection photograph. The reflections from distorted or curved planes form elongated spots. [7].

Laue transmission photographs, like back-reflection photographs, consist of patterns of spots. The arrangement of these spots differ in the two methods. Transmission patterns usually have spots arranged on ellipses, back-reflection on hyperbolas. See (Fig. 11).

Both the Laue transmission technique and the back-reflection technique are used to determine the orientation of crystal lattices. Both methods can also be used to study a phenomenon called asterism. A crystal that has been distorted in some way will have curved lattice planes. These can act in the manner of curved mirrors, giving deformed or elongated spots instead of small circular images of the X-ray beam. A typical Laue pattern of a distorted crystal is shown in Fig. (14). In many cases, analysis of the asterism, or distortion, of the spots in Laue photographs can lead to valuable information concerning the mechanisms of plastic deformation. [7]

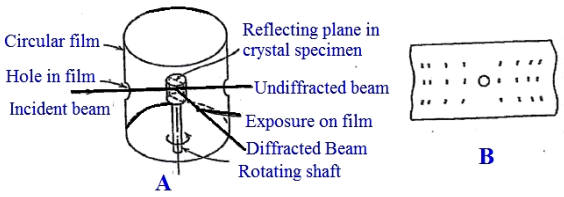

Fig. 14: (A) Schematic diagram of a rotating single-crystal.
(B) Schematic representation of the diffraction pattern obtained from rotating crystal camera. Reflected beams make spots lying in horizontal rows. [7]

In the above examples of Laue methods, the crystal is kept in a fixed orientation relative to the X-

ray beam. Reflections are obtained because the beam is continuous, that is, the wavelength is the variable. Several important X-ray diffraction techniques that use X-rays of a single frequency or wavelength will now be considered. In these methods, since λ is no longer a variable, it is necessary to vary the angle θ in order to obtain reflections.

The Rotating-Crystal Method

In the rotating-crystal method, crystallographic planes are brought into reflecting positions by rotating a crystal about one of its axis while simultaneously radiating it with a beam of monochromatic X-rays. The reflections are usually recorded on a photographic film that is curved to surround the specimen. (See Fig. 17 for a schematic view of this method).[7]

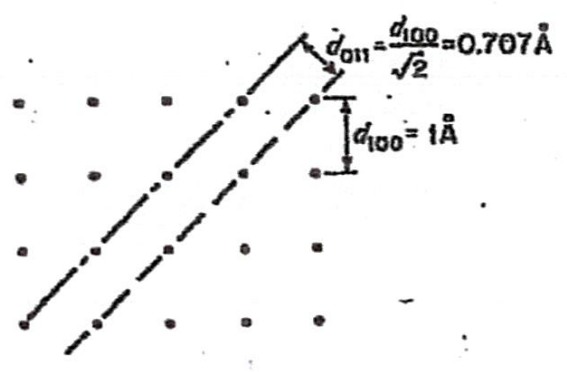

Fig. 15: Simple cubic lattice. Relative interplanar spacing for (100) and (110) planes. [7].

The Debye-Scherrer or Powder Method

In this method the specimen contains more than several hundred randomly oriented crystals. It may consist of either a small polycrystalline metal wire, or a finely ground powder of the metal contained in a plastic, cellulose, or glass tube. In either case, the crystalline aggregate consists of a cylinder about 0.5 mm in diameter with crystals approximately 0.1 mm in diameter or smaller. In this, as in the rotating single-crystal method, the angle θ is the variable while the wavelength λ remains constant. In the powder method, a variation of θ is obtained through the presence of many small crystals randomly oriented in space in the specimen. The principles involved can best be explained with the aid of an example. [7]

"For the sake of simplicity, let us assume a crystalline structure with the simple cubic lattice shown in Fig. (15) and that the spacing between {100} planes equals 1 Å. It is easy to show that the interplanar spacing for planes of the {110} type are equal to that of {100} planes divided by the square root of two, and is, therefore, 0.707 Å. (See Fig. 15). The {110} spacing is, therefore, smaller than the {100} spacing. In fact, all other planes in the simple cubic lattice have a smaller spacing than that of the cubic, or {100}, planes. This is expressed in the equation given below for the spacing of crystallographic planes in a cubic lattice, where *h, k,* and *l* are the three Miller indices of a plane in the crystal, d_{hkl} the interplanar spacing of the plane, and *a* the length of the unit-cell edge.

$$d_{hkl}=\frac{a}{\sqrt{h^2+k^2+l^2}} \qquad (9)$$

In the simple cubic structure, the distance between cubic planes, d_{100}, equals *a*. Therefore, the above expression is written:

$$d_{hkl}=\frac{d_{100}}{\sqrt{h^2+k^2+l^2}} \qquad (10)$$

Now according to the Bragg equation

$$n\lambda = 2d\sin\theta \qquad (11)$$

and for first-order reflections, where *n* equals one, we have

$$\theta = \sin^{-1}\left(\frac{\lambda}{2d}\right) \qquad (12)$$

This equation tells us that planes with the largest spacing will reflect at the smallest angle θ. If it is now assumed that the wavelength of the X-ray beam is 0.4 Å, first-order reflections will occur from {100} planes (with the assumed 1 Å spacing) when

$$\theta = \sin^{-1}\frac{0.4}{2(1)} = \sin^{-1}\frac{1}{5} = 11^\circ\,30' \qquad (13)$$

{100} planes with a spacing 0.707 Å reflect when

$$\theta = \sin^{-1}\frac{0.4}{2(0.707)} = 16^\circ\,28' \qquad (14)$$

All other planes with layer indices (that is, {111}, {234}, etc.) reflect at still larger angles." [7]

In Fig. (16) we see how the Debye-Scherrer reflections are formed. A parallel beam of monochromatic X-rays coming from the left of the figure is shown striking the crystalline aggregate. As

the specimen bear hundreds of randomly oriented crystals, many of these will have {100} planes at the correct Bragg angle of 11°30′. Each of these crystals will reflect a part of the incident radiation in a direction that makes an angle twice 11°30′ with the beam. However, because the crystals are randomly positioned in space, all the reflections will not lie in the same direction. Instead, they will lie along the face of a cone that makes an angle of 23° with the original direction of the X-ray beam. Similarly, it can be shown that first-order reflections from {110} planes form a cone with an angle of twice 16°28′, or 32°56′ with the original direction of the beam. Planes of still higher indices form cones of reflected rays making larger and larger angles with the original direction of the beam.

The most commonly used powder cameras use a long strip film that is curved into a circular cylinder surrounding the specimen, as show in Figure (17a). A schematic view of a Debye-Scherrer film after exposure and development is shown in Figure (17b). [7]

.

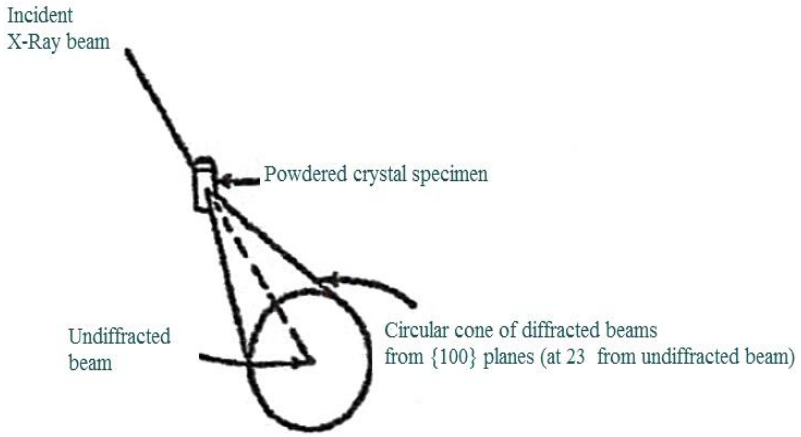

Fig. 16: First-order reflections from (100) planes of a hypothetical simple cubic lattice. Powdered crystal sample. [7]

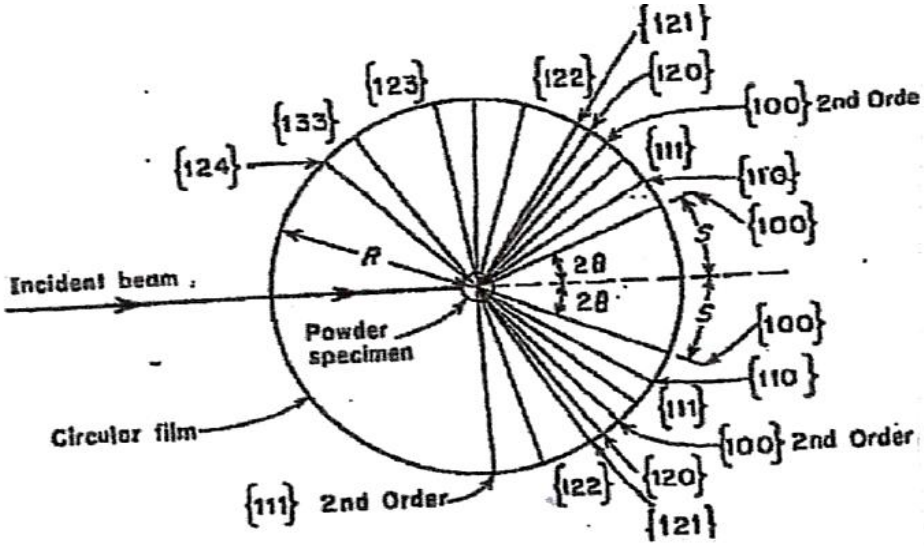

Fig. 17: (a) Schematic representation of the Debye or powder camera. Sample assumed to be simple cubic. Not all reflections are shown. [7].

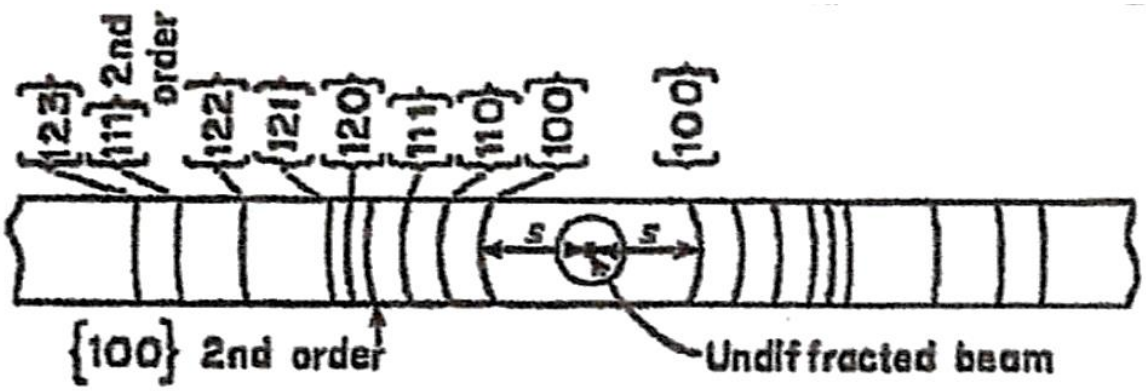

Fig. 17: (b) Powder camera photograph. Diffraction lines correspond to the reflections shown in Fig. 17 (A).

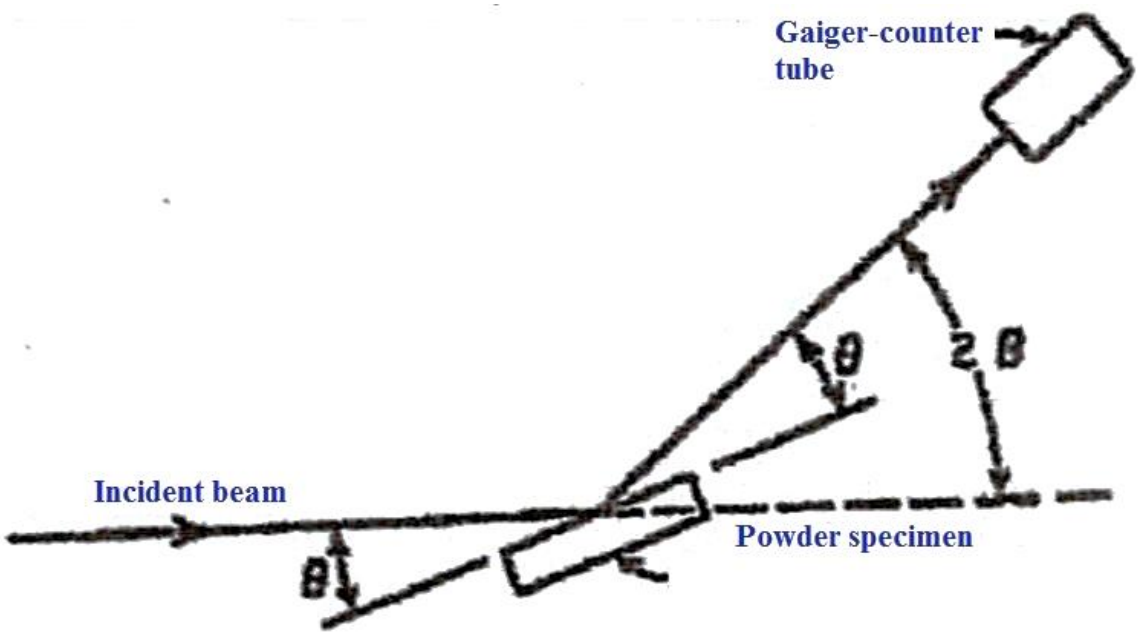

Fig. 18: X-ray spectrometer. [7]

On a Debye-Scherrer film, the distance 2*S* between the two circular segments of the {100} cone is related to the angular opening of the cone and to the Bragg angle θ between the surface of the cone and the X-ray beam, which equals *S/R*, where *R* is the radius of the circle formed by the film. However, this same angle also equals 2θ, so that

$$2\theta = \frac{S}{R} \qquad (15)$$

or

$$\theta = \frac{S}{2R} \qquad (16)$$

This last relationship is important because it makes it possible to measure the Bragg angle θ. In the above example, the spacing between parallel lattice planes was assumed to be known. This assumption was made in order to explain the principles of the Debye-Scherrer method. However, very often the interplanar spacings of a crystal are not known and then measurements of the Bragg angles can be used to calculate these quantities. The powder method is a powerful way of determining the crystal structure of a metal. In complicated crystals, the powder method may have to be used together with other methods. The Debye-Scherrer method is probably the most important of all methods used in the determination of crystal structures. Since each crystalline material has

its own characteristic set of interplanar spacings, the powder method has yet another important application. While copper, silver, and gold all have the same crystal structure (face-centered cubic), their unit cells are different in size, and, therefore, the interplanar spacings and Bragg angles are different in each case. Since each crystalline material has its characteristic Bragg angles, it is possible to identify unknown crystalline phases in metals with the aid of their Bragg reflections. To this end a card file system (X-ray Diffraction Data Index) has been published which lists approximately a thousand elements and crystalline compounds for their Bragg angle of each important Debye-Scherrer diffraction line and its relative strength or intensity. The structural elucidation of an unknown crystalline phase in a metal can be establish by comparing powder pattern Bragg angles and reflected intensities of the unknown substance with the proper card of the index. This method is like a fingerprint identification system and is an important method of qualitative chemical analysis. [7]

The X-ray Spectrometer

The X-ray spectrometer is an instrument that measures the intensity of the X-ray reflection from a crystal with an electronic device, such as a Geiger counter tube or ionization chamber in place of a photographic film. Fig. (18) gives a schematic diagram of a spectrometer consisting of a crystalline specimen, a parallel beam of X-rays, and a Geiger counter tube. The arrangement is such that both the crystal and the Geiger counter tube can 5 rotate. However, the counter tube always moves at twice the speed of the specimen. This ensures that the intensity recording device is at the proper angle during the rotation of the crystal in order to register each Bragg reflection as it occurs. In modern instruments of this type, the intensity measuring device is connected to a chart recorder via an amplification system and the power of the reflection is documented on a chart by a pen. In this way one can obtains an accurate plot of intensity against Bragg angles. A typical X-ray spectrometer plot is shown in Fig. (19).

The X-ray spectrometer is usually used with a powder specimen in the form of a rectangular plate of about 1 in. long and ½ in. wide. The specimen may be a sample of a polycrystalline metal. In contrast to the Debye-Scherrer method where the specimen is a fine wire (approximately 0.5 mm diameter), the spectrometer sample has a finite size. This makes the specimen much easier to prepare and is therefore an advantage. Because the X-ray spectrometer is capable of measuring the intensities of Bragg reflections with great accuracy, it can be used for both qualitative and quantitative chemical analysis. [7]

The Transmission Electron Microscope

Nowadays a very powerful technique is available to metallurgists – the electron microscope (Fig. 20). It can be used to study the internal structure of thin crystalline films or foils. These foils, which can be removed from bulk samples, are normally only several thousand Å thick. The thickness is dictated by the voltage at which the microscope is operated. A normal instrument is rated at about 100,000 volts, which can give an acceptable image provided the foil is not made thicker than the indicated value. A thinner foil will reveal less of the nature of the structure of the metal. Newly developed instruments can operate at voltages of the order of a million volts. For such instruments, the foils can be proportionately thicker. However, the cost of such equipment is much higher so relatively few of these are available. [7]

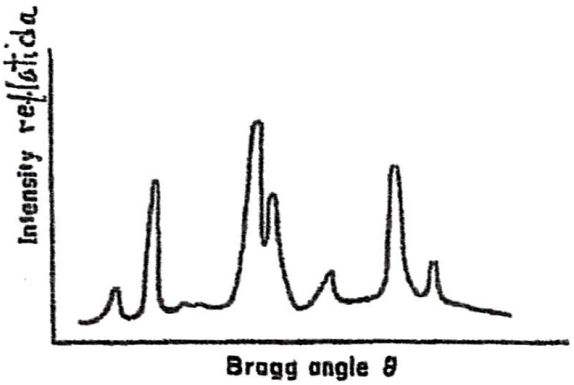

Fig. 19: The X-ray spectrometer records the reflected intensity as a function of Bragg angle on a chart. Each intensity peak corresponds to a crystallographic plane in a reflecting position. [7]

In the transmission electron microscope, the detail image is generated by the diffraction of electrons from the crystallographic planes of the object being investigated. It is, in many ways, similar to an optical microscope. Instead of a light filament, the source is an electron gun. The lenses are magnetic and are made up of a current-carrying coil surrounded by a soft iron case. The lenses are energized by direct current. An excellent, easy to read description of the electron microscope is given in the book by Smallman and Ashbee [8]. For our present purposes we shall concentrate on that part of the microscope containing the specimen and the objective lens. This area is schematically drawn in Fig. (21). Here the electron beam is shown entering the specimen from above. This beam originates in the electron gun and

passes through a number of condensing lenses before reaching the sample. On emerging from the specimen, the beam passes through the rear element of the instrument's objective lens. Slightly beyond this lens element, the rays converge to form a spot at point *a* in plane I_1. This spot is equivalent to an image of the source. Slightly beyond this point, the image of the specimen is formed at plane I_2. Similar double image effects can be observed in simple optical instruments where it is possible to form images of the light source at one position and images of a lantern slide or other object at other positions. [7]

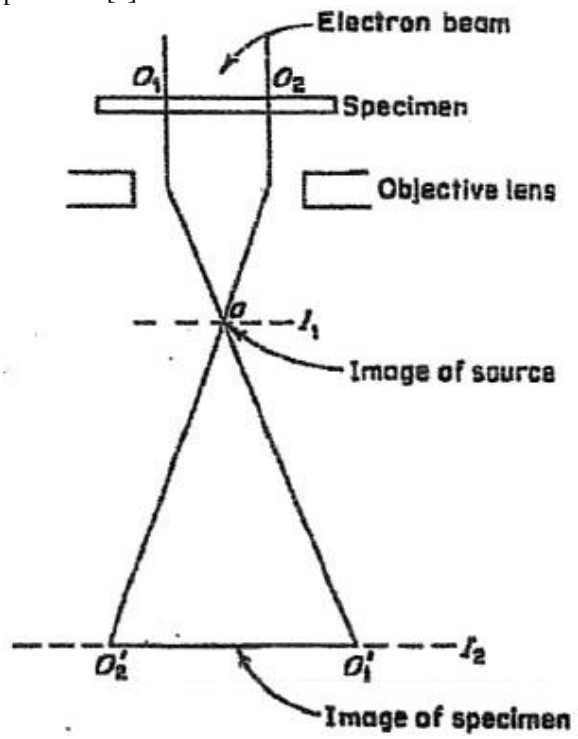

Fig. 20: Schematic drawing of a transmission electronmicroscope. [7].

Because image formation depends on the diffraction of electrons, it is necessary to consider some elementary facts about this type of diffraction. We already know that electrons have both particle and wavelike properties. It will also be shown that the wavelength of an electron is related to its velocity *v* by the relation

$$\lambda = \frac{h}{mv} \qquad (17)$$

where λ is the wavelength of the electron, *m* is its mass, and *h* is Planck's constant equal to 6.63×10^{-27} erg sec. This expression shows that the wavelength of an electron varies inversely to its velocity - the higher the velocity, the shorter the wavelength. [7]

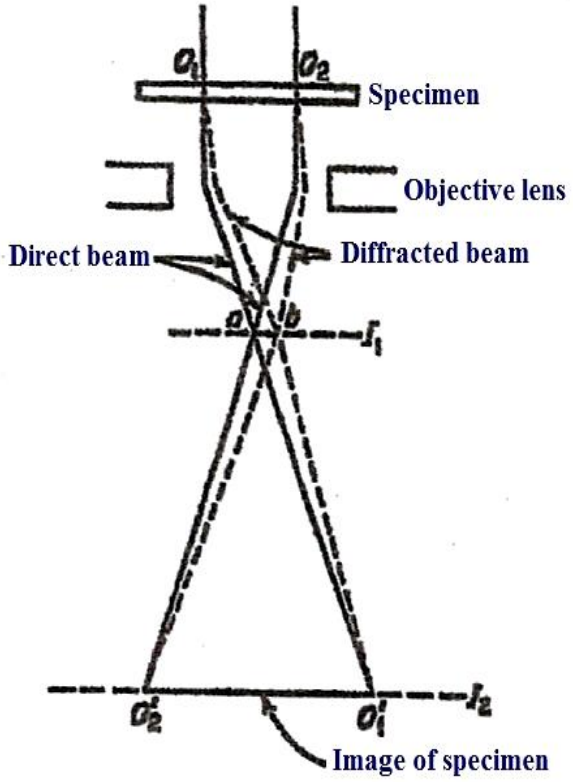

Fig. 21: Images can be formed in the transmission electron microscope corresponding to the direct beam or to a diffracted beam. (Images from more than one diffracted beam are also possible). [7].

Now let us assume that an electron is accelerated by a potential of 100,000 volts. It can easily be shown that this will give the electron a velocity of about 2×10^{10} cm/sec and, by applying the above equation, a wavelength of about 4×10^{-10} cm, or about 4×10^{-2} Å. This is about two orders of magnitude smaller than the average wavelength used in X-ray diffraction studies of metallic crystals. (Fig. 21) This causes a corresponding difference in the nature of the diffraction, as can be deduced by considering Bragg's Law. In first order diffraction, where $n = 1$. Then by Bragg's law, we have

$$\lambda = 2d \sin \theta \qquad (18)$$

If *d*, the spacing of the parallel planes from which the electrons are reflected, is assumed to be about 2 Å, we have

$$\theta \approx \sin \theta = 0.01 \qquad (19)$$

The angle of incidence or reflection of a diffracted beam is thus only of the order of 10^{-2} radius, or about 30′. This means that when a beam of electrons is passed through a thin layer of crystalline material, only those planes nearly parallel to the beam contribute to the resulting diffraction pattern. [7]

We will now look at how the image is formed in the electron microscope as the result of diffraction. It has been assumed that some of the electrons, while passing through the specimen, are diffracted by one of the sets of planes in the specimen. In general, only part of the electrons will be diffracted, the remainder will simply pass directly through the specimen. The latter electrons will form a spot at position *a* and an image of the specimen (O'_2 - O'_1) at the plane I_2, as shown in Fig. (21). The diffracted electrons will enter the objective lens at a slightly different angle and will converge to form a spot at point *b*. The rays that pass through point *b* will also form an image of the specimen at I_2 that is superimposed over that from the direct beam. In the above, it has been assumed that the crystal is so oriented that the electrons are reflected primarily from a single crystallographic plane. This should cause the formation of a single pronounced spot at point *b* as a result of the diffraction. It is also possible to have simultaneous reflections from a number of planes, in which case, rather than a single spot appearing in I_1 at point *b*, a typical array of spots or a diffraction pattern will form on plane *I*. We will now take a closer look at a characteristic diffraction pattern. [7]

The electron microscope is constructed in such a way that, either the image of the diffraction pattern (formed at I_1) or the image of the detail in the specimen (formed at I_2) can be viewed on the fluorescent screen of the instrument. Both of these images can be also be photographed on a plate or film. This is possible because a projection lens system (not shown) is located in the microscope below that part of the instrument shown in Fig. (22). This lens system can be adjusted to project either the image of the diffraction pattern at plane I_1, or that of the specimen at I_2. [7]

When using the instrument as a microscope, either the image formed by the direct beam or the image formed by diffraction from a particular set of planes can be used. Elimination of the beam causing either type of image can be achieved by inserting an aperture diaphragm at plane I_1. This allows only one of the beams to pass through, as shown in Figure (22). In this diagram, the diffracted beam is shown intercepted by the diaphragm, while the direct beam is allowed to pass through the aperture. When the sample is viewed like this, a bright-field image is formed. Imperfections in the crystal will normally appear as dark areas in this image. These imperfections could be small inclusions of different transparency from the matrix crystal, which then become visible in the image due to loss in intensity of the beam where it passes through the more opaque particles. Of greater interest is when the imperfections are faults in the crystal lattice itself. A very important defect of this type is a dislocation. Dislocations involve distortions in the arrangement of the crystal planes. Such local distortions will have effects on the diffraction of electrons, because the angle of incidence between the electron beam and the lattice planes around the dislocation are altered. In some cases this may cause an increase in the number of diffracted electrons and in others a decrease. Since the direct beam can be considered to be the difference between the incident beam and the diffracted beam, a local change in the diffracting conditions in the specimen will be reflected by a corresponding alteration in the intensity recorded in the specimen image. Dislocations are visible in the image because they affect the diffraction of electrons. In a bright-field image, dislocations normally appear as dark lines. A typical bright-field photograph is shown in Fig. (23). [7]

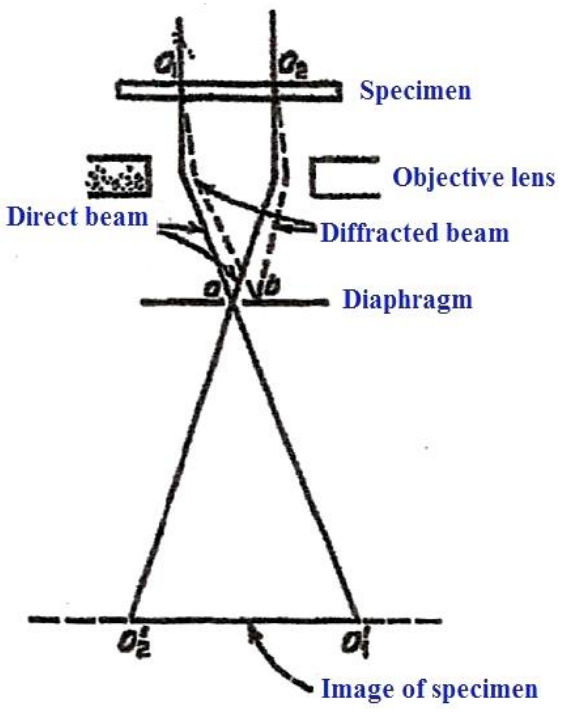

Fig. 22: The use of a diaphragm to select the desired image. [7]

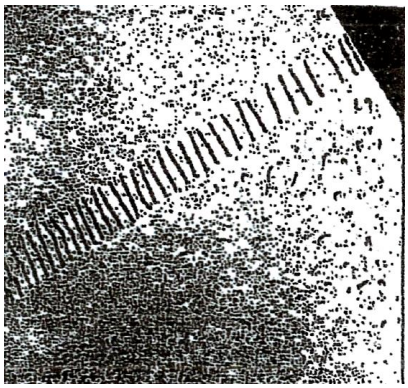

Fig. 23: An electron micrograph of a foil removed from an aluminium sample. (Photograph courtesy of E.J. Jenkins and J. Hren). [7].

Another way of using the electron microscope is to place the aperture in such a way that a diffracted ray is allowed to pass through while the direct beam is cut off. The image of the specimen formed in this case is of the dark-field type. Here, dislocations appear as white lines on a dark background. Bright-field illumination is preferable because dark-field images are usually more subject to distortion. This is because (as may be seen in Fig. 22) the diffracted beam, after leaving the specimen, does not travel down the microscope axis. [7]

An important feature of the transmission electron microscope is the stage that holds the specimen. Since diffraction plays a very important role in making the defects in the crystal structure visible, it is necessary to hold the sample in specific positions so that a suitable crystallographic plane can be brought into a reflecting position. This usually means that it is necessary for the specimen to be tilted with respect to the electron beam. The stage of an electron microscope used for metallurgical investigations is normally constructed in such a way that the specimen can be rotated or tilted. [7]

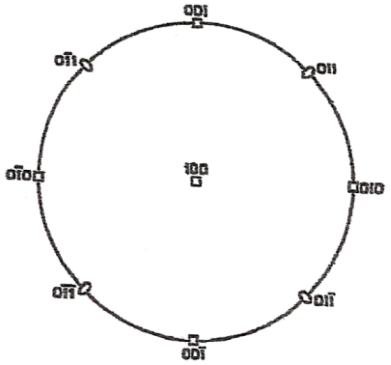

Fig. 24: This stereographic projection of a cubic crystal shows the principle planes whose zone axis is (100). [7].

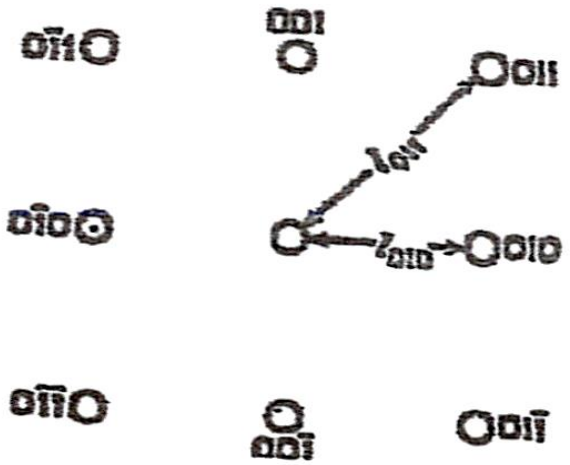

Fig. 25: The diffraction pattern corresponds to a beam directed along (100) in a cubic crystal. [7].

An interesting diffraction pattern is obtained when the specimen is tilted in such a way that an important zone axis is placed parallel to the microscope axis. In such a case, a pattern is formed in which spots correspond to the planes of the zone whose axis is parallel to the electron beam. We will assume that the specimen is oriented so that a < 100 > direction is parallel to the instrument axis. Fig. (24) shows a stereographic projection in which the zone axis is located at the center of the projection. The poles of the planes belonging to this zone should therefore lie on the basic circle of the stereographic projection. Only planes of low indices are shown in the figure. The diffraction pattern corresponding to this zone is shown in Fig. (25). The Miller indices of the planes responsible for each spot are indicated alongside the corresponding spots. [7]

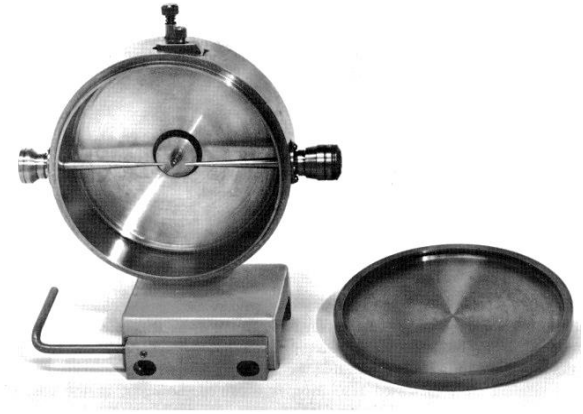

Fig. 26: Hull/Debye-Scherrer camera, with cover plate removed. (Courtesy of Philips Electronic Instruments, Inc.) [11]

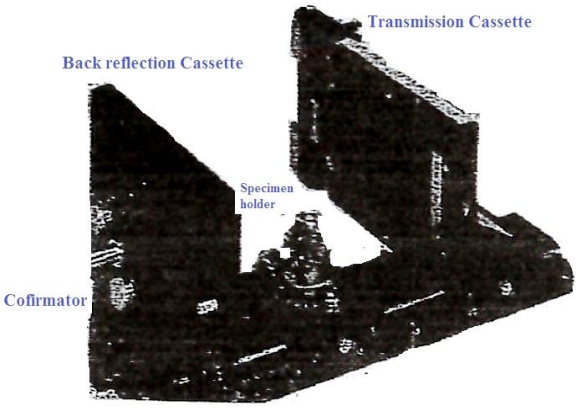

Fig. 27: Combination transmission and back-reflectionLaue camera. In this camera the Polaroid cassette (at right) and the cassette for ordinary film (at left) are interchangeable; either can be used for transmissionor for back reflection. (Courtesy of Blake Industries, Inc) [11]

The most significant fact of the diffraction pattern in Fig. (25) is that all the spots correspond to an axis that is similar to the electron beam. Furthermore, spots are indexed at both 100 and $\bar{1}00$. This implies that the electrons are reflected from both sides of the same planes. It is obvious that the simple Bragg picture shown in Figure (8), where the angle of incidence equals the angle of reflection, does not apply in this case. The reasons for this are not easily understood. Several factors are involved. The low value of the Bragg angle θ, which is of about 10^{-2} radius, is of some importance. Also important is the fact that the transmission specimen is very thin, so that the electron beam, interprets it as a lattice that is nearly two-dimensional. This tends to relax the diffraction conditions. Finally, the electron microscope, with the specimen located inside a system of lenses, is not a simple diffracting device. For our present purposes, however, it is more important to note the nature of the diffraction pattern than the causes for it. [7]

Let us now look at the spacing of the spots in the diffraction pattern in Fig. (25). The distance from the spot corresponding to the direct beam to that of a reflection from a {100} plane is indicated as 1_{010}, while the corresponding distance to a {110} reflection is 1_{011}. As can be deduced from the figure, $1_{001} = \sqrt{2}\ 1_{010}$. From Fig. (17), we saw that the spacing between the two respective planes varies inversely as $\sqrt{2}$. This means that the spacing of the spots in the diffraction pattern is inversely proportionate to the interplanar spacing. This result, unlike the relationship of the incident beam to the planes from which it is reflected, is in agreement with the Bragg law. In the present case, where the angle θ is small, $\sin\theta \approx \theta$ and Bragg's law reduces to

$$n\lambda = 2d\theta \quad (20)$$

or

$$\theta = \frac{n\lambda}{2d} \quad (21)$$

Since the angle θ is small, $\tan\theta$ is also approximately equal to θ and one can expect the diffracted spots to be elucidated through distances that are inversely proportional to the interplanar spacing d. [7]

The above discussion clearly shows that the electron microscope can be used as an instrument to establish the internal defect structure of a crystalline specimen as well as a diffraction instrument to give information about the crystallographic features of the specimen. In the latter case, the diffraction patterns can yield information about the nature of the crystal structure and about the orientation of the crystals in a specimen. Furthermore, the electron microscope has a diaphragm in its optical path that controls the size of the area that is able to contribute to the diffraction pattern. This makes it possible to obtain information about an area of the specimen that has a radius as small as 0.5μ. The diffraction patterns are therefore called *selected area diffraction patterns.*" [7,8] (Fig. 22) Figs. 28-46 show various apparatus and methods used in X-ray diffraction.

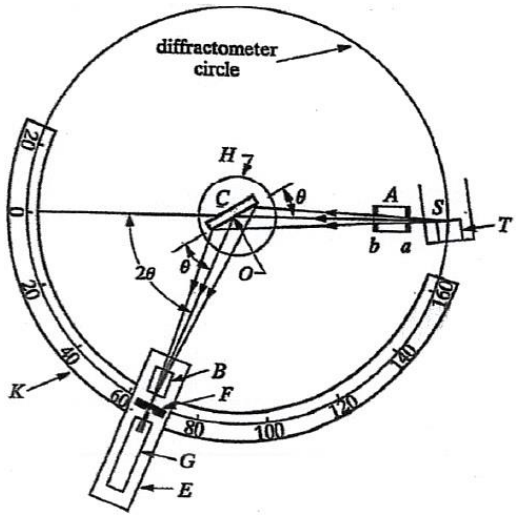

Fig. 28: X-ray diffractometer (schematic). [11].

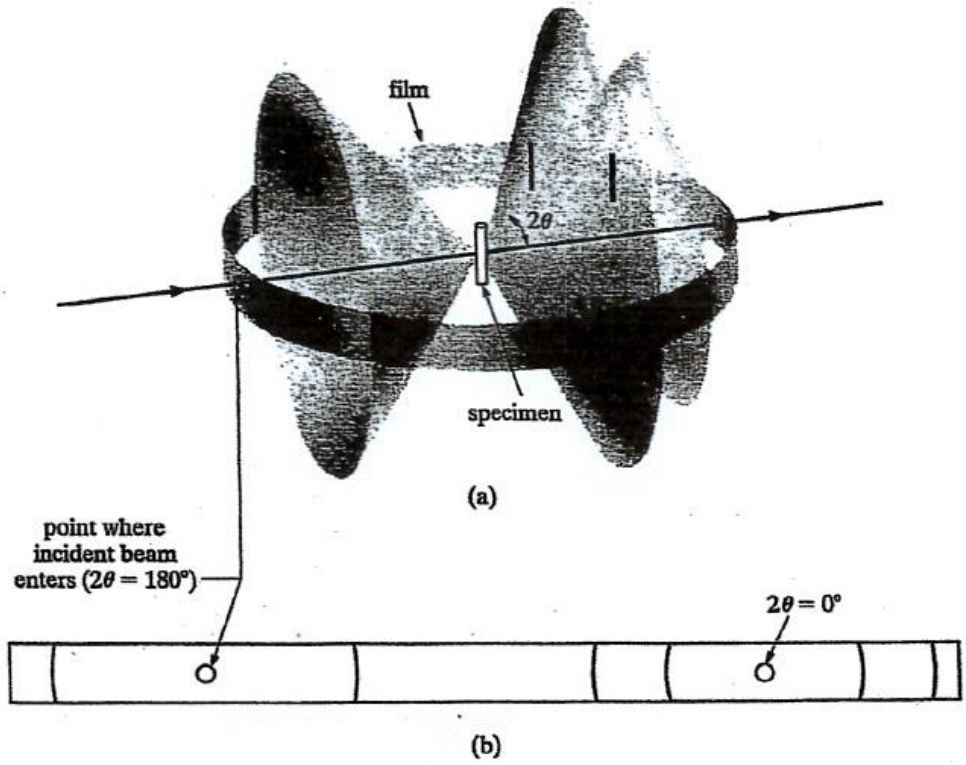

Fig. 29: Hull/Debye-Scherrer powder procedure: (a) relation of film to sample and incident beam. (b) appearance of film when laid flat. [11].

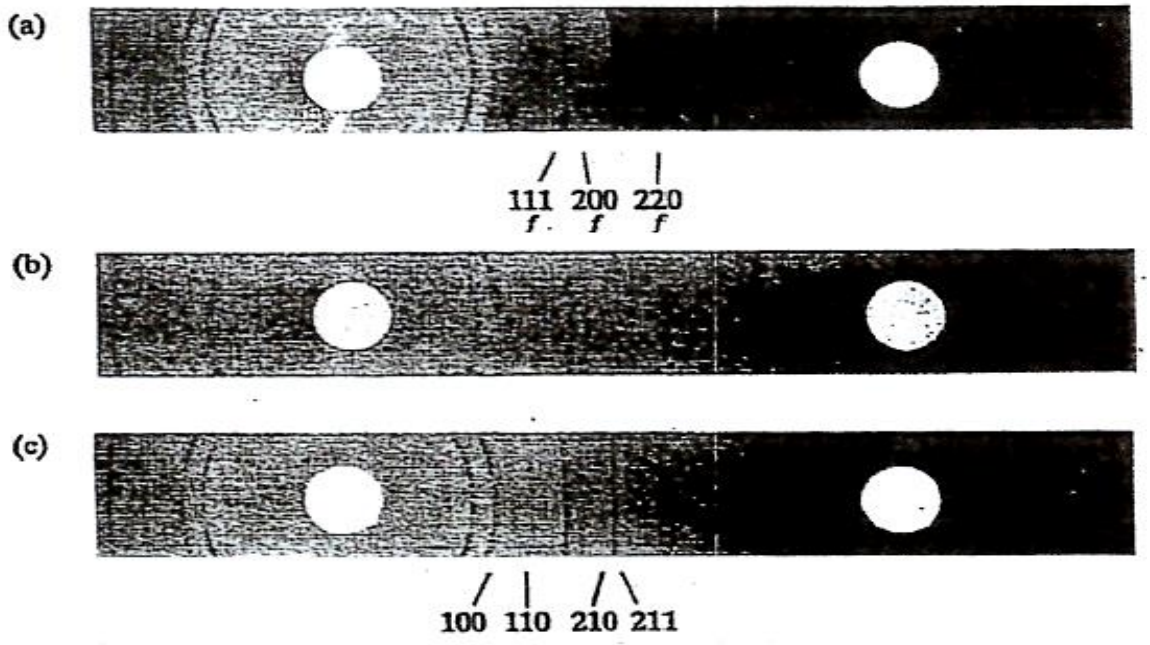

Fig. 30: Hull/Debye-Scherrer powder patterns of copper (FCC), tungsten (BCC) and zinc (HCP). Filtered copper radiation, camera diameter = 5.73 cm. [11].

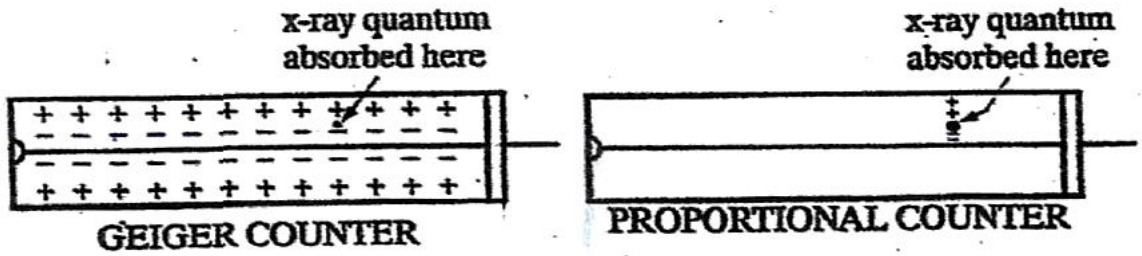

Fig. 31: Differences in the extent of ionization between proportional and Geiger counters. Each plus (or minus) symbol represents a large number of positive ions (or electrons). [11].

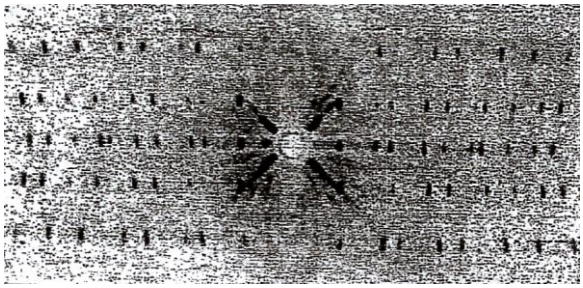

Fig. 32: Rotating-crystal pattern of a quartz crystal (hexagonal) rotated about its ***c*** axis. Filtered copper radiation. (The streaks are due to the white radiation not removed by the filter.) (Courtesy of B.E. Warren.) [11].

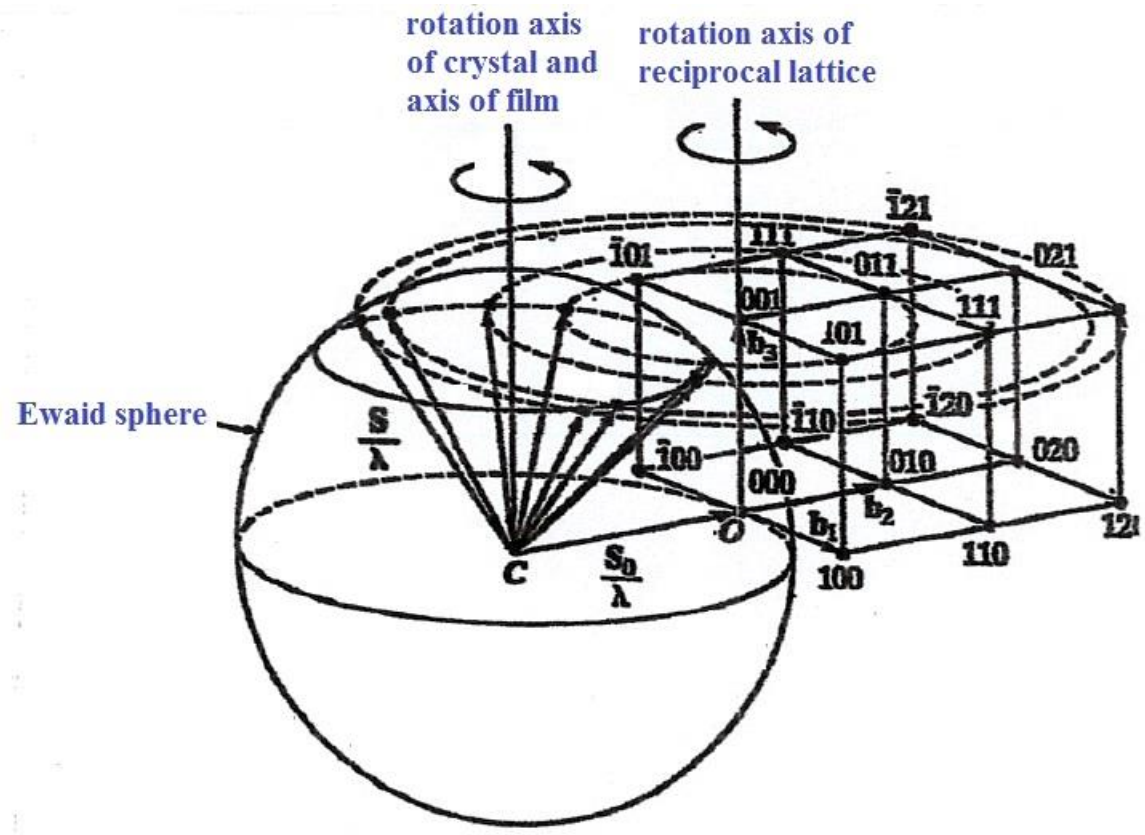

Fig. 33: Reciprocal-lattice treatment of rotating-crystal procedure. [11].

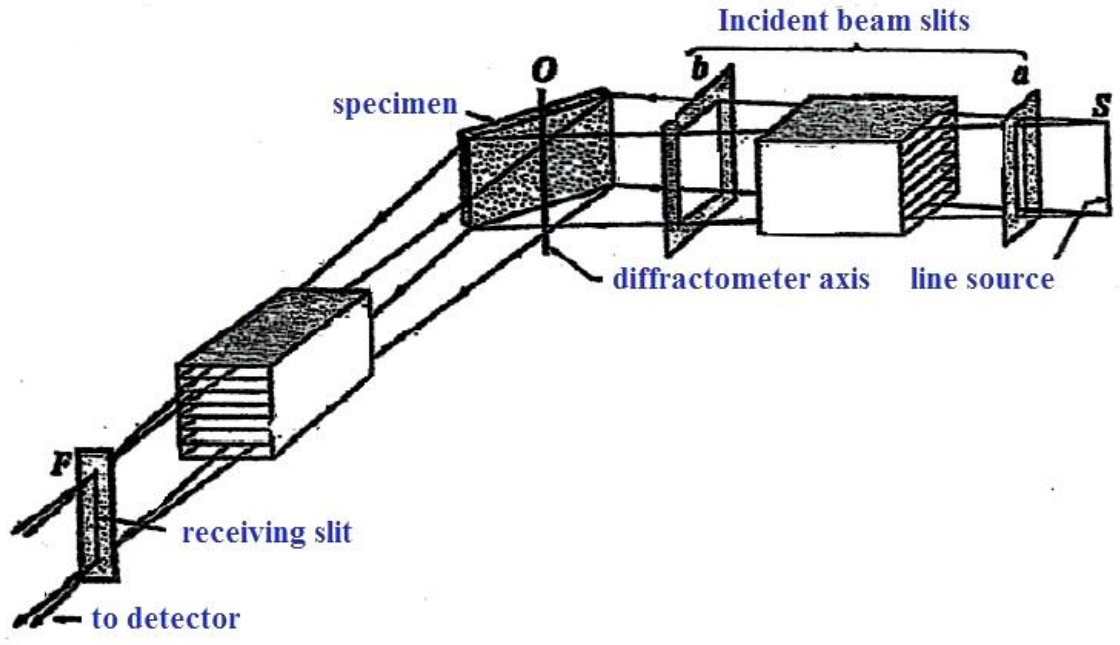

Fig. 34: Arrangement of slits in diffractometer. [11].

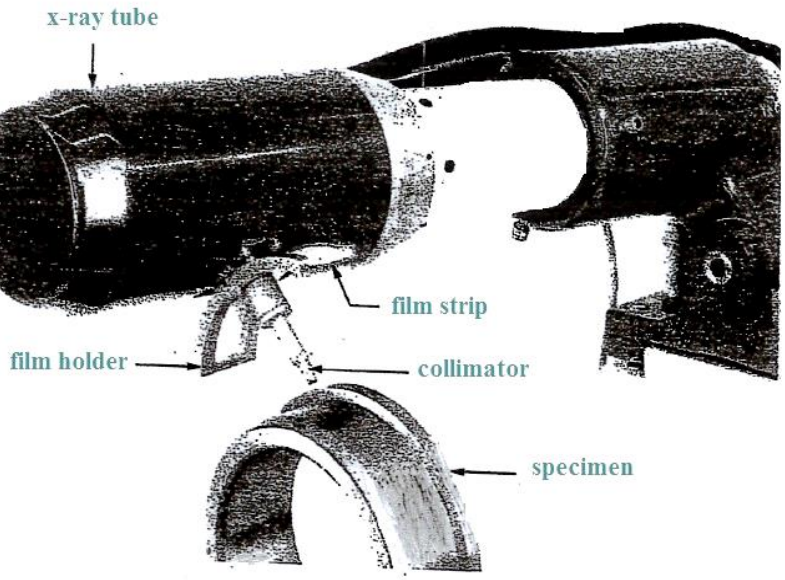

Fig. 35: Stress camera in position for a stress measurement by the single-exposure technique. The head of the x-ray tube is enclosed in a protective cover. (Courtesy of Advanced Metals Research Corporation.) [11].

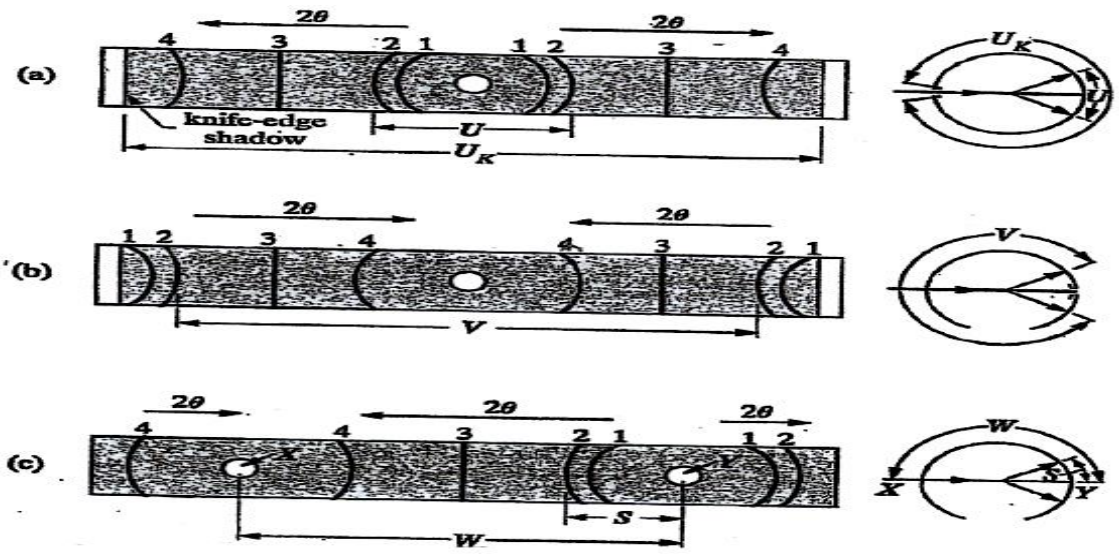

Fig. 36: Procedures of film loading in Hull/Debye-Scherrer cameras. Corresponding lines have the same numbers in all films. [11].

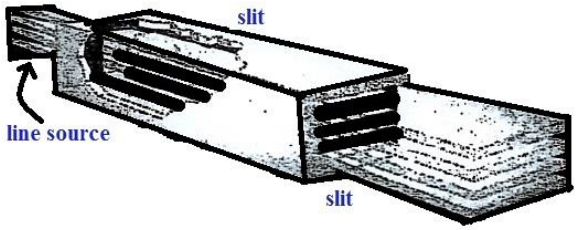

Fig. 37: Soller slit (schematic). For simplicity, only three metal plates are shown; actual Soller slits contain about a dozen. [11].

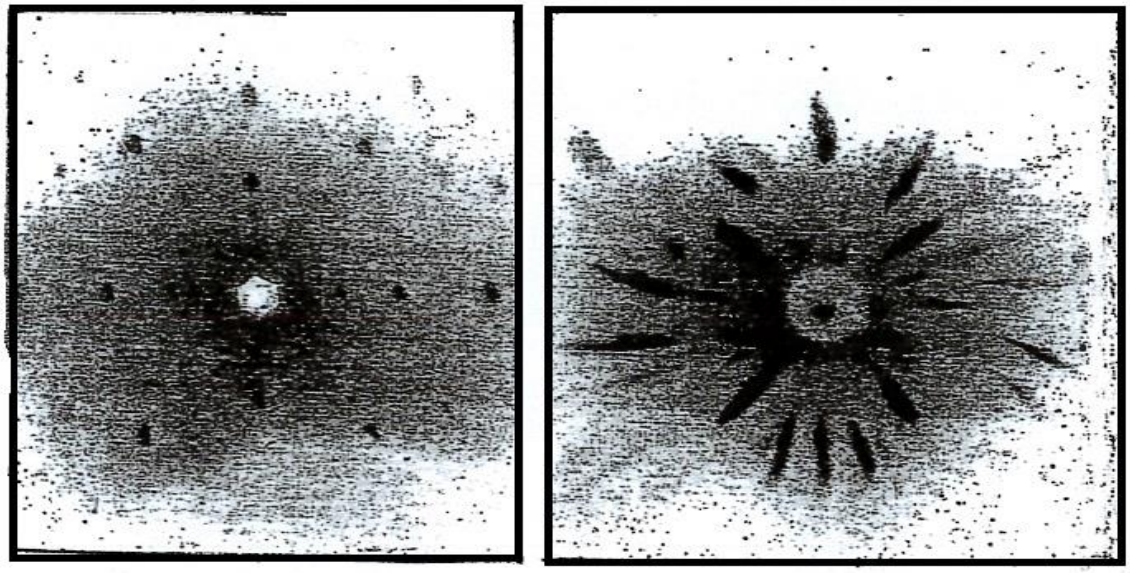

Fig. 38: Laue photographs of a deformed aluminium crystal. Sample-to-film distance 3 cm, tungsten radiation, 30 kV. [11].

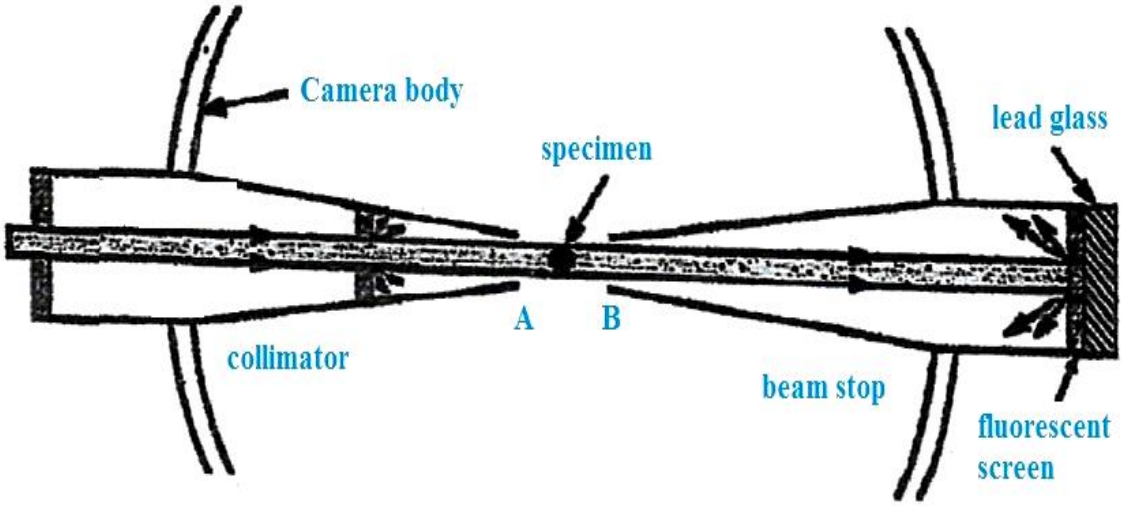

Fig. 39: Design of collimator and beam stop (schematic). [11]

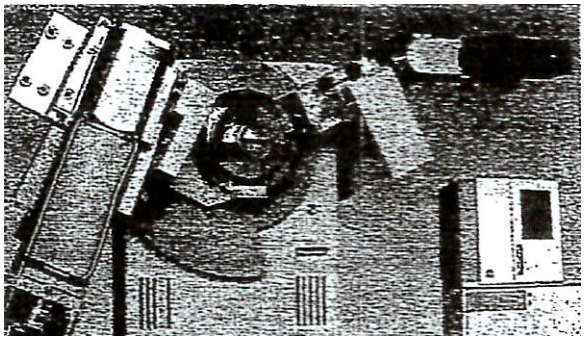

Fig. 40: Rigaku diffractometer. The x-ray tube is at the left and the inset photograph shows the radiation enclosure and PC controlling the dif-fractometer motions. (Courtesy Rigaku) [11].

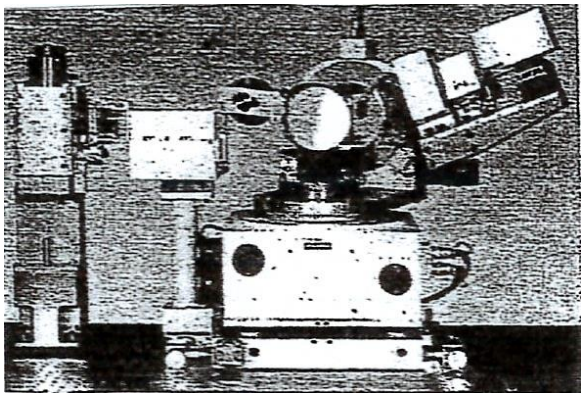

Fig. 41: A second configuration of the Rigaku diffractometer shown in Fig. 98. Here additional sample rotations are possible. (Courtesy Rigaku) [11]

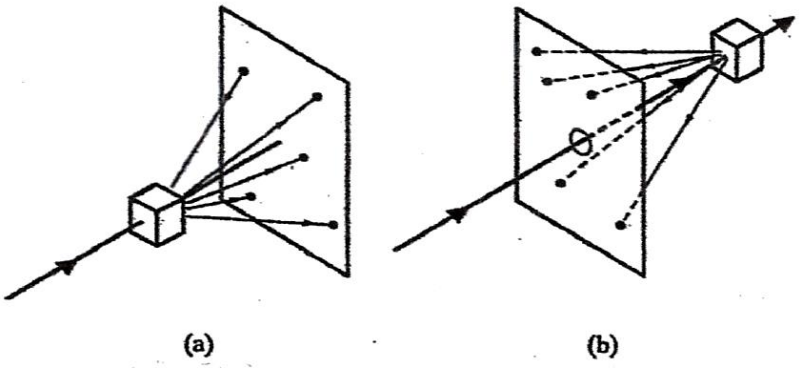

Fig. 42: (a) Transmission and (b) back-reflection Laue procedures. [11].

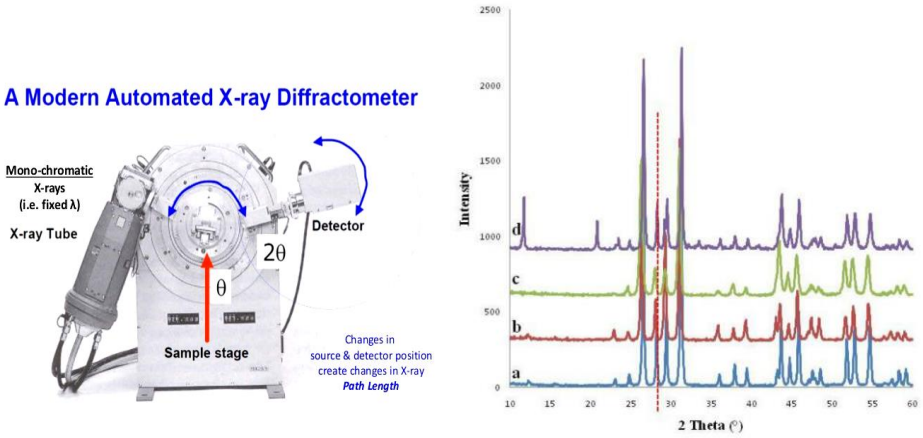

Fig. 43: A modern x-ray diffractometer. [31].

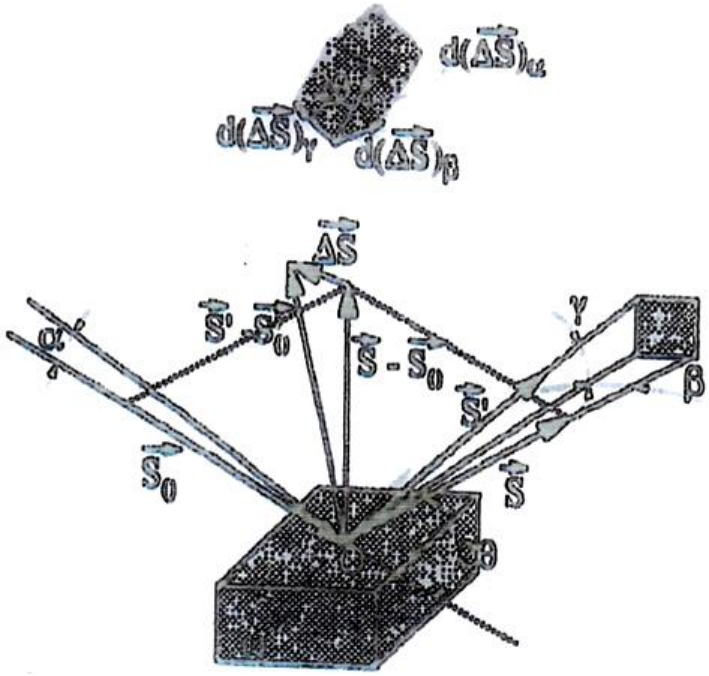

Fig. 44: Diffracting power of an ideal crystal. [20].

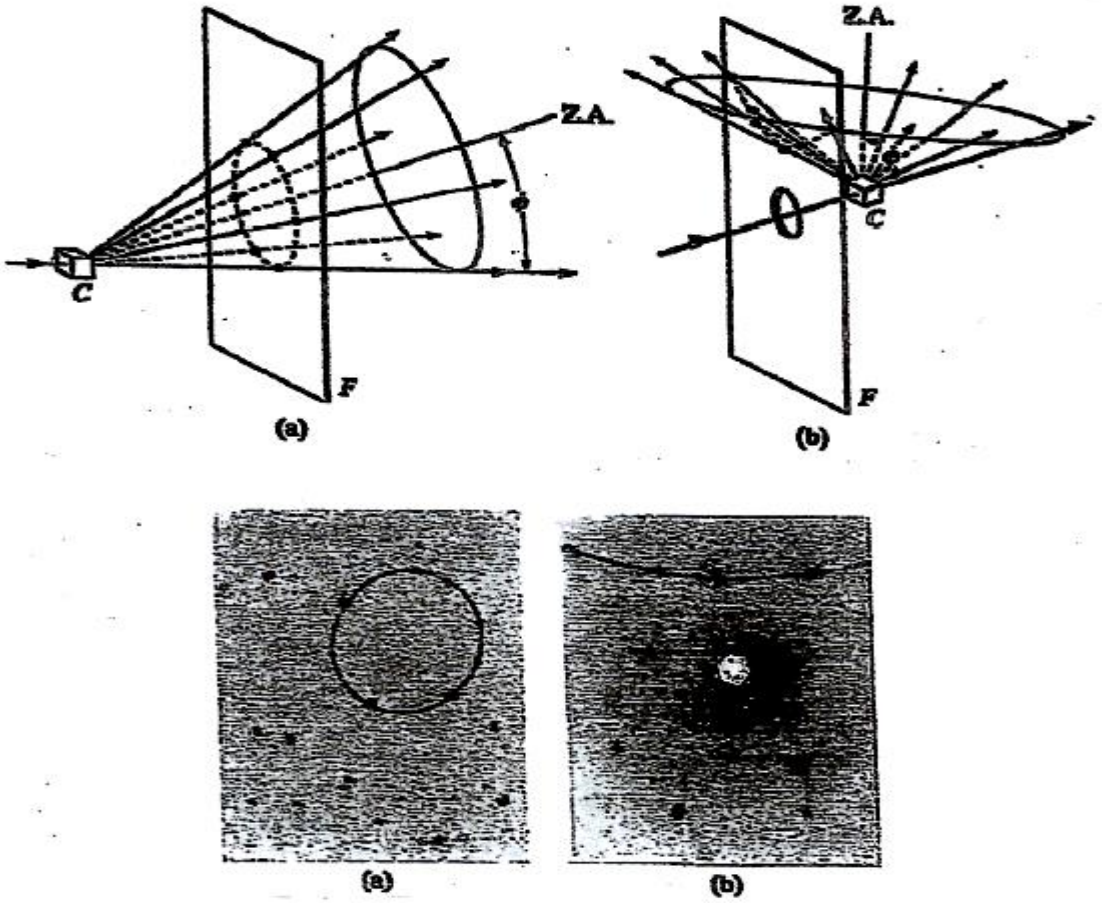

Fig. 45: (a) Transmission and (b) back-reflection Laue patterns of an aluminium crystal (cubic). Tungsten radiation, 30 kV, 19 mA. [11].

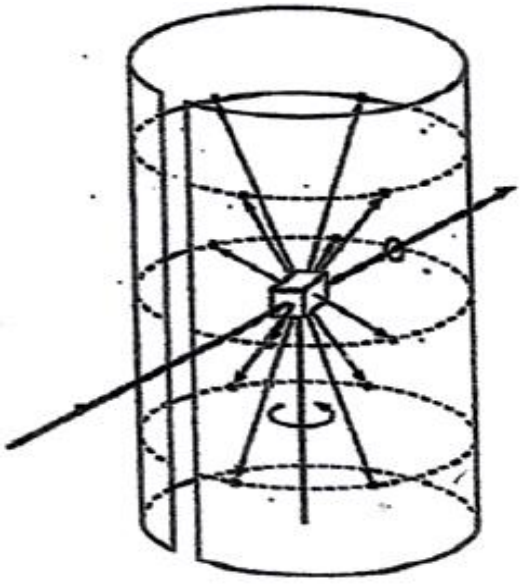

Fig. 46: Rotating-crystal procedure. [11].

Use of X-ray Diffraction in Materials Science [9]

More than 90% of all solid materials can be considered to be crystalline. When interacting with a crystalline substance (phase), X-rays create diffraction patterns. Crystalline substances all give a pattern – the same substance always gives the same pattern. In an alloy, each component produces an individual pattern. At this time, about 50000 inorganic and 25000 organic single component crystalline phase diffraction patterns have been collected and stored on magnetic or optical media as standards.

X-ray diffraction can be used to determine

(1) The composition phase in a sample during quantitative phase analysis such as the comparative amounts of phase in a mixture by comparaing the relative peak intensities.
(2) Bravais lattice symmetry and unit cell lattice parameters and.
(3) position of index peaks.
(4) The parameters lattice can vary as a function of alloying elements and therefore generating information about, doping, alloying, solid solutions, strains, etc.
(5) Residual strain (macrostrain).
(6) Crystal structure – Rietveld refinement of the whole diffraction pattern.
(7) Epitaxy / texture / orientation.
(8) microstrain and Crystallite size – revealed by peak broadening - other defects (stacking faults etc.) can be measured by analysis of peak shapes and peak width.
(9) Evaluation of all properties as a function of time, temperature and gas environment, etc. etc. [9]

X-ray Crystallography

X-ray crystallography is defined as the scientific method used for determining the sequence of atoms in a crystalline solid in three-dimensional space. This technique makes use of the interatomic distance of most crystalline solids by taking them as a diffraction gradient for X-ray light, that has a wavelength to the order of 1 angstrom (10^{-8} cm). [10]

In 1895, Wilhelm Röntgen discovered X-rays and scientists were puzzled whether X-rays were particles or electromagnetic radiation which was a hot topic of discussion until 1912. If one could have accepted the wave idea then the wavelength of this light must have been in the range of 1 Angstrom (Å) (10^{-8} cm). Measurement and diffraction of such wavelengths must have a gradient with spacing on the same order of magnitude as light.

In 1912, Max Von Laue, at the University of Munich in Germany, proposed that atoms in a crystal lattice had periodic and regular structure with interatomic distances of about 1 Å. Lacking any evidence to support his claim, he further proposed that the crystalline structure can diffract X-rays, just like a gradient diffract infrared light in an infrared spectrometer. His assumptions were based on the following: the atomic lattice is periodic in a crystal, X-rays radiation are electromagnetic in nature, and the interatomic distance of a crystal are of the same magnitude as X-ray light. Laue's predictions were verified by Friedrich and Knipping who easily photographed the diffraction pattern associated with the X-ray radiation of crystalline $CuSO_4 \cdot 5H_2O$ and thus the science of X-ray crystallography start flourishing. [10]

Atoms need to be arranged in a periodic structure in order to diffract the X-ray beams. Mathematical calculations are then applied to produce a diffraction pattern which is characteristic for that particular arrangement of atoms in that crystal. Even to this day, X-ray crystallography remains the primary tool to characterize the structure and bonding in organometallic compounds. [10]

After the pioneering work of Von Laue on diffraction by crystals, the Braggs (father and son) did research of vital importance and put X-ray crystallography on a solid footing. Max Von Laue was awarded the Nobel Prize for Physics in 1914 and the Braggs in 1915.

Many materials form crystals – minerals, salts, metals, semiconductors, organic, inorganic and biological molecules, etc. X-ray crystallography has, therefore, become important in the progress of many scientific fields. Within the first decade of its use, this method established the size of atoms, the types and lengths of chemical bonds, and the atomic-scale differences between various materials, especially minerals and alloys. This method also confirmed the structure and function of many natural molecules, such as drugs, vitamins, proteins and nucleic acids such as DNA. It is still the main method for establishing the atomic structure of new materials. X-ray crystal structures is also responsible for unusual elastic or electronic properties of a material, shed light on chemical interactions and processes [10]

For X-ray diffraction measurement of a single-crystal, it is mounted on goniometer. This is used to hold the crystal at selected orientations. The crystal is then illuminated with a finely focused

monochromatic beam of X-rays, which produces a diffraction pattern of regularly spaced spots known as *reflections.* These two-dimensional images that have been taken at different orientations are then transformed into a three-dimensional model of the density of electrons in the crystal using the mathematical method of Fourier transformations, combined with the chemical data known for the sample. Poor resolution (fuzziness), or even errors, can result from crystals that are too small, or not uniform enough in their internal makeup. [10]

"X-ray crystallography is not the only method for determining atomic structures. Such kind of diffraction patterns can also be generated by scattering electrons or neutrons, which are then also interpreted by Fourier transformation. If single crystals of sufficient size cannot be generated, other X-ray methods are available, but these give less detailed information; these include powder diffraction and fiber diffraction, (for non-crystalline material) small-angle X-ray scattering (SAXS). If the material under research is only exist in the form of nanocrystalline powders or displays poor crystallinity, the methods of electron crystallography can be used for establishing the atomic structure. [10]

Among all the afore-mentioned X-ray diffraction methods, the scattering is flexible; the scattered X-ray having the same wavelength as the incoming X-ray. [10]

Reference [10] gives a lot of information on the cultural and aesthetic importance of X-ray crystallography, its contributions to chemistry and materials science, mineralogy and metallurgy, early organic and small biological molecules, biological macromolecular crystallography and on other X-ray techniques, methods of single-crystal X-ray diffraction, X-ray sources, procedures and limitations.

Use of Fourier series in structural analysis

"A *Fourier series* is a kind of infinite trigonometric series through which any kind of periodic function can be expressed. The one important property of a crystal is that its atoms are distributed in space in a regular manner. This also suggests that the density of electrons is also a periodic function of position in the crystal, elevating to the point where an atom is located and coming down to a low value in the region between atoms. To regard a crystal as a positional variation of electron density compared to an arrangement of atoms, is especially suitable where diffraction is involved because X-rays are scattered by electrons and not by atoms. As the electron density is a periodic function of position, a crystal may be described analytically by means of the Fourier series. This is very useful in structure determination because it can be shown that the coefficients of the various terms in the series are related to the [F] values of the various X-ray reflections. But such a series cannot be used immediately, since the structure factors are not usually known both in magnitude and phase. However, another kind of series has been devised - the Patterson function - whose coefficients are related to the experimentally observable [*F*] values and which gives, not electron density, but information regarding the various interatomic vectors in the unit cell. This information is often enough to establish the phase of the various structure factors, then the Fourier series can be used to map out the real electron density in the cell and thus disclose the atom position. [11]

Fourier analysis and Fourier transform theory are the mathematical tools that provide the formal link to the NMR imaging application, which is strikingly similarity to that of the other very high-resolution imaging tool which have been of traditional importance to the chemist, viz., X-ray crystal structure analysis. The cell of a single crystal contains the molecular structure information that chemists want to know. From the physics of experimentation, we know that the observed intensity data set - scattered X-rays - is related to the structure of the sample by applying the three-dimensional Fourier transform. [11]

Example of structure determination

(Courtesy Cullity (1978) Addison Wesley Publishing Co., Reading, Mass (USA) and Cullity, Stock and Pearson India Educational Services, Noida (U.P.), India, Second Edition (2015), we are reproducing the following information) - [11]

Here we are considering an intermediate phase which can be found in the cadmium-tellurium system. Chemical analysis of the material revealed essentially one phase under the microscope, it contain 46.6 weight percent Cd and 53.4 weight percent Te. This is equivalent to 49.8 atomic percent Cd and can be represented by the formula CdTe. The specimen was reduced to powder and a diffraction pattern obtained with a Hull/Debye-Scherrer camera (Fig. 26) and Cu $K\alpha$ radiation. Moreover, Fig. 27 shows an important combination of a transmission and back reflection Laue camera which can be used for both transmission and X-ray diffraction photographs. Important information about various pieces of equipment and methods of X-ray diffraction, both for scientific and medical purposes, are given in Figs. 28 – 46 and 47 – 53 respectively.

The observed values of $\sin^2\theta$ for the first 16 lines are listed in Table 1, together with the visually estimated relative line intensities. This pattern can be indexed on the basis of a cubic unit cell, and the indices of the observed lines are given in the table. The lattice parameter, calculated from the $\sin^2\theta$ value for the highest-angle line, is 6.46 Å.

The density of the specimen, as determined by weighing a quantity of the powder in a pyknometer bottle, was 5.82 g/cm^3.

$$\sum A = \frac{(5.82)(6.46)^3}{1.66042} = 945. \quad (22)$$

Table-1: Observed values of $\text{Sin}^2\theta$ for the first 16 lines of CdTe sample.

Line	Intensity	$\text{Sin}^2\theta$	*hkl*
1	s	0.0462	111
2	vs	0.1198	220
3	vs	0.1615	311
4	vw	0.1790	222
5	m	0.234	400
6	m	0.275	331
7	s	0.346	422
8	m	0.391	511,233
9	w	0.461	440
10	m	0.504	531
11	m	0.575	620
12	w	0.616	533
13	w	0.688	444
14	m	0.729	711,551
15	vs	0.799	642
16	s	0.840	731,553

"Since the molecular weight of CdTe is 240.02, the number of "molecules" per unit cell is 945/240.02 = 3.94, or 4, within experimental error.

Knowing that the unit cell of CdTe is cubic and that it contains 4 "molecules" of CdTe, i.e., 4 atoms of cadmium and 4 atoms of tellurium, possible arrangements of these atoms in the unit cell can be evaluated. Examination of the indices listed in Table 5 reveals that the indices of the observed lines are all unmixed and that the Bravais lattice must be face-centered. (Not all possible sets of unmixed indices are present, 200, 420, 600, 442, 622 and 640 are missing from the pattern. These reflections may be too weak to be observed, and the fact that they are missing does not invalidate the conclusion that the lattice is face-centered.) Now there are two common face-centered cubic structures of the AB type, i.e., containing two different atoms in equal proportions, and both contain four "molecules" per unit cell: these are the NaCl structure and the zinc-blende form of ZnS. Both of these are logical possibilities even though the bonding in NaCl is ionic and in ZnS covalent, since both kinds of bonding have been observed in telluride structures.

The next step is to calculate relative diffracted intensities for each structure and compare them with experiment, in order to determine whether or not one of these structures is the correct one. If CdTe has the NaCl structure, then its structure factor for unmixed indices is given by

$$F^2 = 16(f_{Cd} + f_{Te})^2, \text{if } (h+k+l) \text{ is even} \quad (23)$$

$$F^2 = 16(f_{Cd} - f_{Te})^2, \text{if } (h+k+l) \text{ is odd} \quad (24)$$

On the other hand, if the ZnS structure is correct, then the structure factor for unmixed indices is given by

$$|F^{\uparrow}2| = 16(f_{\downarrow}Cd^{\uparrow}2 + f_{\downarrow}Te^{\uparrow}2)), \text{if } (h+k+l) \text{ is odd,} \quad (25)$$

$$|F^2| = 16(f_{Cd} - f_{Te})^2, \text{if } (h+k+l) \text{ is an odd multiple of 2,} \quad (26)$$

$$|F^2| = 16(f_{Cd} + f_{Te})^2, \text{if } (h+k+l) \text{ is an even multiple of 2.} \quad (27)$$

Even before making a detailed calculation of relative diffracted intensities by means of the NaCl structure can almost be eliminated as a possibility simply by inspection of Esq. (27). The atomic numbers of cadmium and tellurium are 48 and 52, respectively, so the value of $(f_{Cd} + f_{Te})^2$ is several hundred times greater than the value of $(f_{Cd} - f_{Te})^2$, for all values of $(\sin\theta)/\lambda$. Then, if CdTe has the NaCl structure, the 111 reflection should be very weak and the 200 reflection very strong. Actually, 111 is strong and 200 is not observed. Further evidence that the NaCl structure is incorrect is given in the fourth column of Table 2, where the calculated intensities of the first eight possible lines are listed: there is no agreement whatever between these values and the observed intensities.

On the other hand, if the ZnS structure is assumed, intensity calculations lead to the values listed in the fifth column. The agreement between these values and the observed intensities is excellent, except for a few minor inconsistencies among the low-angle reflections, and these are due to neglect of the absorption factor. In particular, note that the ZnS structure satisfactorily accounts for all the missing reflections (200, 420, etc), since the calculated intensities of these reflections are all extremely low. Therefore this sample of CdTe has the structure of the zinc-blende form of ZnS.

Following a given arrangement has been publicized to be in according with the diffraction

information, it is suitable to estimate the interatomic gaps occupied in that arrangement. This estimation not only is of concern in itself other than to reveal any gross faults which may have been complete, since there is clearly something incorrect with a planned composition if it carry certain atoms insufferably close collectively. In the present structure, the adjacent neighbor to the Cd atom at 0 0 0 is the Te atom at $\frac{1}{4}\frac{1}{4}\frac{1}{4}$. The Cd-Te interatomic gap is therefore a/4 = 2.80 Å. For comparison a "theoretical" Cd-Te interatomic distance can be found simply by averaging the distances of closest approach in the clean elements. The atoms treat as rigid spheres in contact and ignore the effects of coordination number and type of bonding on atom size is ignored. These distances of closest approach are 2.98 Å in pure cadmium and 2.86 Å in pure tellurium, the average being 2.92 Å. The observed Cd-Te interatomic distance is 2.80 Å, or some 4.1 percent smaller than the calculated value; this variation is not unreasonable and can be largely credited to the covalent bonding which characterizes this structure. Actually, it is a general rule that the A-B interatomic distance in an intermediate phase A_xB_y is always somewhat smaller than the average distance of closest approach in pure A and pure B, because the mere existence of the phase show that the attractive forces between unlike atoms is higher than that between like atoms. If this were not true, the phase would not form." [11]

Table-2:

1	2	3	4	5
Line	Hkl	Observed Intensity	Calculated Intensity*	
			NaCl structure	ZnS structure
1	111	s	0.05	12.4
	200	nil	13.2	0.03
2	220	vs	10.0	10.0
3	311	vs	0.02	6.2
4	222	vw	3.5	0.007
5	400	m	1.7	1.7
6	331	m	0.01	2.5
	420	nil	4.6	0.01
7	422	s	……	3.4
8	511,333	m	……	1.8
9	440	w	……	1.1
10	531	m	……	2.0
	600,422	nil	……	0.005
11	620	m	……	1.8
12	533	w	……	0.9
	622	nil	……	0.004
13	444	w	……	0.6
14	711,551	m	……	1.8
	640	nil	……	0.005
15	642	vs	……	4.0
16	731,652	s	……	3.3

*Calculated Intensities have been adjusted so that the 220 line has an intensity of 10.0 for both structures.

When an annealed alloy is cold perfor,med, its diffraction lines become harder. This is quite established, simply verified experiments reality, as its details were since many years a matter of controversy. Some investigators felt that the chief effect of cold work was to fragment the granules to a point where their small size alone was sufficient to account for all the observed broadening. Others accomplished that the nonuniformity of strain produced by cold work was the major cause of broadening, with granule fragmentation possibly a minor contributing cause. This argument revolved about the quantity of line widths and their clarification in conditions of either "particle-size broadening", as per "strain broadening".

"In 1949/1950, although, Warren [11] find out that there were significant particulars with the reference the condition of a cold-worked metal in the *shape* of its diffraction lines, and that to base end only on line *width* was responsible only division of the experimental evidence. If the practical line profiles, corrected for instrumental expansion, are eloquent as Fourier series, after that an analysis of the Fourier coefficients discloses equally particle size and strain, with no requirement for any preceding supposition as to the continuance of [11-13]. Warren and Averbach [14] complete the first quantity of this kind, on brass filings, as well as many alike studies to follow. Later, Paterson [15, 16] demonstrates that the Fourier coefficients of the line profile might also express the incidence of stack fault basis by cold work. (In FCC metals and alloys, as, slip on {111} planes can here and there change the normal heaping sequence *ABCABC…* of these panes to the fault sequence *ABCBCA….*) Therefore three reasons of line broadening are finally identified: small crystallite size, no uniform strain, and stacking faults." [11]

"This study of line shape shows that it was likely to simplify about the reasons of line broadening in cold-worked metals and alloys. In a few materials all three causes give, in others only one." [11]

"The broadening of a diffraction line by buckle cannot always be observed by simply examination of a photograph or a diffractometer scan but for some standard is available for comparison. On the other hand, the separation of the $K\alpha$ doublet furnishes a very good "internal standard". In the back-reflection region, a relatively strain-free material produces a well-resolved doublet, one part as $K\alpha_1$ radiation and another to $K\alpha_2$. For a certain set of experimental situations, the division of this doublet is stable and free of the quantity of microstrain. However as the quantity of deformation is maximum, the broadening amplifies, as finally the two parts of the doublet partly cover to such an amount that they demonstrate as one unsettled line. An unsettled $K\alpha$ doublet can consequently be taken as proof of cold work; if the similar doublet is determined as the material is in the annealed or strain-free state." [11]

For more information on the application of Fourier series to crystal structure consult Robertson [17], Sneddon [18], Guinier [19], Guinebretiere [20], Titmarsh [21], Clegg [22], Lipson and Cochran [23], Chatterjee [24] etc. etc.

Important developments

The vast progress in theory and techniques had two instant, far-reaching consequences for the discipline of X-ray crystallography. In the initial position, the theoretical foundation now well-known for the understanding of strengths of X-ray reflections complete it probable for the Fourier procedure of study to be put into a working quantitative type. And Compton made the most important step by deriving Fourier series expression from first principles, to introduce the quantitative appearance for the structure feature, and shows accurately how the coefficients are connected to X-ray intensities. In 1929 W. L. Bragg extended the procedure more and complete utilization of a double Fourier series for the earliest time, to apply the results to his study of the diopside crystal. With many experimental difficulties solved by Bragg and his colleagues lots of structures of vast difficulty were totally solved, viz., those of Inorganic Chemistry and Physics of the Solid State usually, were obtaining. Later, Krishnan and Banerjee, Lonsdale and others developed auxiliary procedures of great importance. Other procedures of great importance were developed by Patterson and West using direct Fourier series. The paper by Robertson [17] describes these two important developments.

Patterson procedure

Patterson's direct procedure of study was established in 1935. A dissimilar form of Fourier sequence was in work, which represented a subjective standard division of density concerning any position in the crystal. The coefficients are relative to the squares of the structure features and are in dependent of the phase constants. The results can provide precious information concerning definite interatomic gaps in the crystal. [17, 23, 24] A detailed description of the Patterson procedure is given by René Guinebretière [20] and Chatterjee [24]

West procedure

A brilliant, more direct procedure for determination of crystal structure using Fourier series provide by West in 1930. An introduction Fourier production to employ certain deposit of reflection provide a number of signs of Oxygen atoms in potassium dihydrogen phosphate. These approximately determined positions then enable the time constants of the further sets of reflection to be considered. Frequently application of Fourier syntheses then led to a whole and precise purpose of the structure.

Mainly straight pictures of complex structures, though, obtain through the study of definite isomorphons sequence of crystals; contain some changeable element in a particular location. This element can be substitute for significantly distressing the residue of the structure. The result of production such a replacement is to replace the complete values of the structure features by a identified amount but in a direction depending on the phase stability of the reflection. Therefore, to observe the directions of this change, a direct purpose of the phase constants can be complete and a straightforward Fourier synthesis of the structure is carry out. [17]

Practical application of Fourier series

Some crystal structure of a Fourier sequences, it's necessary to keep in mind to the sequences are only convergent as the coefficients of the maximum terms low in magnitude. It is obvious from Fig. 27 that at bigger look angles there is maximum interference amongst the sprinkled rays. So the values of *F* and the coefficients in the sequences do turn into smaller for terms connecting high indices. The quantity of decreasing off, but depends on how much the electron division is intense on the crystal plane. In a structure consisting of single atoms, the division is very intense near the centers, if the atoms are at rest. But at normal temperatures the atoms have substantial thermal motions and the electron distribution is efficiently much more spread, conclude that at great glancing angles the intensities of the diffracted beams drop off rapidly.

This consideration is important while interpreting the conclusions of a Fourier synthesis. It is believed that we can't go to measure the coefficients of the sequences without letting up – a restriction is place by the experimental circumstances, mainly with the wave-length of the radiation use. Therefore, the limiting glancing angles of 90° correspond to a least amount spacing of $\lambda/2$ by equation. (28) At this time if the coefficients of the Fourier sequences are yet huge when it is completed by the experimental circumstances, serious limitations will occur in the density division which represent. This defect takes the variety of fake description and region of negative density which have no physical sense. This substance has been considered by Havighurst [17] for single Fourier sequences, and by Bragg and West [25] for

double Fourier series. The latter authors make an exciting contrast of the protuberance obtain by double Fourier sequences with the container of the image produced by an optical instrument with a circular end, and illustrate that the defects in the Fourier projection of a crystal are same to those formed by optical diffraction. If θ_0 is the limiting glancing angle equal to which the spectra are calculated, they explain that the numerical opening in X-ray study must be clear as 2 sin θ_0, and that description cannot be illustrious if not it is on a coarser scale than $0.6\ \lambda/2 \sin \theta_0$.

When the Fourier sequences is developed for a known crystal, preventive measures is required in noting the path in which the phase stable varies in the dissimilar quadrants of the reciprocal lattice, where the numerical values of the structure features may be the same. It depends on the regularity. The valuable step of functioning out all same relations totally for all the gaps groups and summing the terms for the electron density in general the quadrants has newly been concluded by Lonsdale. [17]

To determine every structure features of a known crystal creates it achievable to find out *a priori* the worth taken by the dispersal factor at any position of the crystal cell and finally it is likely by contrast to find out the nature of the dispersion atoms.

This kind of reading, commonly refer to as structural analysis, gives two issues:

(a) The strength diffracted by the family of plane with indices (hkl) is comparative to the square modulus of the structure feature;
(b) Only a definite number of reflections (hkl) should be calculated and so the Fourier series is restricted. [20].

Rietveld crystal structure refinement procedure

Constructing a reasonable structural model is done in a different way depending on whether or not same structures are known. It is usually in diffraction by polycrystalline samples to suggest a structural model by analogy with known structures that serve as references. In this situation, a new structure conceives by changing the atoms, which modify the values of their integrated intensities. The structural model is recognized by taking into account consideration involving the nature and the length of the interatomic bonds, ionic radii, etc. The structure is then refined by using procedures described below.

One more approach consists of starting directly with the results of the diffraction measurements and generating a structural model without any reference considerations; the procedure which mentioned as *ab initio*[24]. The last approach is same as to the one commonly used for structural analysis whose measurements are made with single crystals. It needs a considerable amount of data, of course. The name of the procedure depends on how the structural model is built: it is known to as the direct procedure [25] when the model is directly recognized after estimation, for each peak, the modules of the corresponding structure factor, and as the Patterson procedure [26] if representations of the associated Patterson function are used.

Refinement procedures, whether applied to structural determination in order to obtain more information, generally rely on the same plan: they consist of minimizing, by the help out of an algorithm, the gap between a theoretical and an experimental graph. When the refinement performs with the objective of determining the structure of the diffracting crystals, the parameters that can be refined are these structural parameters (nature and positions of the atoms, thermal agitation and occupation rates). At the end of the 1960s, Rietveld [27] suggested a general procedure to conduct the whole pattern fitting of diffraction patterns.

The works of Rietveld [24] led to significant progress in structural analysis from polycrystalline samples. A huge number of inorganic materials and, more advanced organic materials were thus resolved. In 1993, a book edited by Young [28] was written exclusively on the subject of this procedure. In the 1990s, the International Union of Crystallography Commission on Power Diffraction arranged two international tests on this procedure [29]. There are a lot of programs existing today designed for this kind of study and even though this procedure is used by a emerging number of researchers, it remains not easy to apply and require a gradual approach toward the result.

Readers involved will find a complete presentation of Rietveld refinements, with every step describe in detail, in [20, 24].

Bragg's Pioneering Contribution

It is attractive to know that it was W. H. Bragg who in 1915, when present the Bakerian Lecture to the Royal Society, developed for the first time [11] the plan of the application of Fourier series to the issue of X-ray analysis. The continuation of the crystal means a certain reliability of structure; some unit of pattern which can scatter X-rays must be

repetitive in a periodic way over a various range. Any such periodic distribution of the density of the scattering matter may be analyzed by Fourier's procedure into a series of harmonic terms, and it can be shown that each X-ray reflection corresponds to one of these component sinusoidal distributions of density in the medium. Bragg [11] realizes that the coefficients of the Fourier series which represented the periodic variation of density in the medium should be proportional to the intensities of the corresponding X-ray reflections, but this procedure was not put into a useable quantitative form because of many uncertain factors. Later Ewald, Darwin and Compton made absolute measurements showing that the theoretical formulae were fundamentally correct.

Favoured Orientation

"Several applications of X-ray diffraction need exact, accurate information of the lattice parameter of the material in investigation. These applications primarily involve solid solutions (solid materials), since the lattice parameters of a solid solution vary with the concentration of the solute, the composition of a given solution can be determined from a measurement of its lattice parameter. Thermal expansion coefficients can also be found, without a dilatometer, by measurements of lattice parameter as a function of temperature in a high-temperature camera or diffractometer. Since, in normal, a change in solute concentration produces only a little change in lattice parameter, rather precise parameter measurements should be made to measure these quantities with any precision.

The procedure of measuring a lattice parameter is indirect one, and is luckily of such a nature that high precision is quite easily obtained. The parameter $\boldsymbol{a}$ of a cubic substance is directly proportional to the spacing $\boldsymbol{d}$ of any particular set of Bragg planes. Measuring the Bragg angle $\boldsymbol{\theta}$ for $\boldsymbol{hkl}$ and using Bragg's law to find out $\boldsymbol{d}$ allows calculation of $\boldsymbol{a}$. But it is sin $\boldsymbol{\theta}$, not $\boldsymbol{\theta}$, which appear in Bragg's law. Precision in $\boldsymbol{d}$, or $\boldsymbol{a}$, therefore depends on precision in sin $\boldsymbol{\theta}$, a derived quantity, and not on precision in $\boldsymbol{\theta}$, the measured quantity. This is luckily due to the value of sin $\boldsymbol{\theta}$ changes very minor with $\boldsymbol{\theta}$ in the neighborhood of 90^o. For this reason, a very precise value of sin $\boldsymbol{\theta}$ can be obtain from a measurement of $\boldsymbol{\theta}$ which is itself not particularly accurate, *provided that* $\boldsymbol{\theta}$ *is near* 90^o. For example, an error in $\boldsymbol{\theta}$ of 1^o lead to an error in sin $\boldsymbol{\theta}$ of 1.7% at $\boldsymbol{\theta}$ = 450 but only 0.15% at $\boldsymbol{\theta}$ = 850. [18]

"For quantitative phase analyses, the quality of the structure determination is related to limits set on the modifications of the diffracted intensity, caused by preferential orientation effects. This issue, which is specific to diffraction on pollycrystalline samples, generally constitutes one of the limitations of the studies on these types of samples and deserves consideration, particularly in the case of structural studies.

The number of crystals comprising the sample has to be very high and their orientation has to be random. It sometimes happens, however, that this condition is impossible to fulfill, resulting in discrepancies between the integrated intensities of the peaks in the pattern and the values related to structural parameters. When the nature of this preferential orientation is known, it is probable to take it into account in the refinement. This led several authors to incorporate, into their Rietveld refinement programs, preferential orientation parameters based on the use of the March function which was first introduced by Dollase [11]. Nonetheless, it is still better to avoid any texture effects." [11]

"Favored orientation is a normal state. Amongst metals and alloys it is the majority clear in wire and sheet, and the types of surface found in these goods are to treat below. The favored orientation that is formed by the producing process itself (wire drawing or sheet rolling) is known as *deformation texture*. It is because of the propensity of the granules in a polycrystalline collective to rotate throughout plastic bend; each granules undergo slide and rotation in a intricate method that is find out with the compulsory forces and with the slip and rotation of adjacent granules; the result is superior, non-random orientation. As the cold-worked metal, obsessed of a bend surface, is re-crystallized by annealing, the new granule structure usually has a favored orientation too, frequently dissimilar from that of the cold-worked substance. It is known as *recrystallization texture* or *annealing texture.* Due to the influence about the texture of the cold-worked matrix has on the nucleation and/or growth of the novel granules in the matrix." [11]

"Favored orientation is not restricted to metallurgical goods. It subsists too in rocks, in ceramics, in semiconductor thin films and other coatings and in equally natural and artificial polymeric fibers as well as sheets. Actually, favoured orientation is usually the law, not the exemption, and the research of an collective with totally casual crystal orientations is a hard substance." [11]

"The industrial value of favoured orientation lies in the result, actually very noticeable, which has on the whole, macroscopic capabilities of substances.

Given the reality as all single crystals, have dissimilar properties in diverse ways, it tracks that a collective having preferential orientation should have also directional capabilities to a higher or lower degree. Such capabilities might or might not be helpful, depends on the proposed use of the substance. As, sheet steel for the cores of little electric motors could have, for magnetic ways, all granules oriented with their {100} planes similar to the sheet plane. Other than this texture won't be acceptable but the steel were to be produced into a cup by deep illustration; at this time a texture with {111} planes similar to the surface will create the steel fewer same to break during the severe bend of deep illustration; But, if the division to be produced by deep illustration has an asymmetrical form, a still dissimilar texture, may give in better results. A number of controls of texture are likely by the good choice of formation variables as degree of bend and annealing temperature, but metallurgists don't still appreciate surface creation sound enough to form any preferred surface in any exacting metal at will." [11].

"Because of its technological importance, the literature on observed textures and any texture prediction is extensive. Here the focus is on the nature of texures and by their purpose by X-ray procedures. Detailed coverage of the various techniques, special experimental procedures and computational techniques appear elsewhere." [11, 25, 26]

The oldest and most widely used procedure is that proposed by L.G. Shulz in the Journal of Applied Physics (20, 1030) 1949 under the title: "A Direct Procedure of Determining Favoured Orientation of a Flat Reflection Sample Using a Geiger Counter X-ray Spectrometer. [27]

Use of X-ray diffraction in medicine [28]

Immediately after the discovery of X-rays by Röntgen in 1895 and his demonstration of the X-ray photo of the hand of his wife using X-rays, the medical doctors were the first to use it enthusiastically to check broken bones and stones etc in kidneys, livers etc. The dentists started using it to check cavities in teeth.

The science of radiation protection – Health Physics

Now-a-days detectors, dosimeters, monitors are widely used in nuclear laboratories, nuclear plants. The Radiation Monitoring grows out of the similar discoveries of X-rays and Radioactivity in the ending 5 years of the 19^{th} century. Experimenters, physicians, laymen and physicists set-up X-ray to generate apparatuses and formed about their labors with lack of concentration reference to potential danger. This was due to the knowledge that there was nothing in previous experience to suggest that X-rays were hazardous. However, the widespread and uncontrolled use of X-rays led to serious injuries. In the beginning, X-rays were not suspected of any injury but some early experiments did tie X-ray exposure and skin burn together. Thomas Edison, William J Morton and Nikola Tesla were first to report eye exasperations from X-rays and fluorescent substances. "Nowadays, it can be said that radiation ranks investigated for the origin of diseases. On the basis of thorough and many investigations a certain radiation level was prescribed to protect workers in industries, hospitals and nuclear plants." [28]

What are medical X-rays?

(National Institute of Biomedical Imaging and Bioengineering – X-rays)

"X-rays another kind of of electromagnetic radiation, same as to visible light. Dissimilar light, therefore X-rays have high energy and be able to move from side to side the objects, as well as the body. Medical X-rays are responsible to form shapes of tissues and structures within the body. If X-rays moving within the body too move by an X-ray detector in another hand of the tolerant, a picture will be made which characterizes the "shadows" produced by the objects within the body.

Another kind of X-ray detector is photographic film, but many new kinds of detectors which are responsible to generate digital shapes. The X-ray shapes in resultant from this procedure known as radiographs." [29]

How medical X-rays working?

To form a radiograph, an object is placed in order that the division of the body be shaped is consisting between an X-ray resource and an X-ray detector. As the machine is plugged on, X-rays moves in the body and captivated in various amounts by many other tissues depend on the radiological density of the tissues they move. Radiological density is finding out the density and atomic number both the material being shaped. As exemplar, structure such as bone contains calcium that has a maximum atomic number than mainly tissues. Due to this asset, bones gladly suck up X-rays and, therefore, formed maximum difference on the X-ray detector. Finally, bony shapes emerge whiter than tissues against the black surroundings of a radiograph. On the contrary X-rays moves further simply by less radiological thick

tissues for example fat and muscle, and by air-filled body. The shapes are display in the shade of gray under radiograph. [29]

At what time medical X-rays working?

The given examination and procedures that responsible X-ray technology to also identify [29]

Diagnostic [29]

X-ray radiography: Identified bone breaks, certain lump and other irregular masses, pneumonia, several kinds of injury, calcifications, foreign objects, dental issues, etc.

Mammography: A radiograph of the breast which is responsible for cancer identification. Lumps likely look as equal or unequal images of bodywhich are slightly different in color than the surroundings on the radiograph. Mammograms identify small bit of calcium, called microcalcifications that shows brilliant speck on mammogram. It may rarely point out the occurrence of definite kinds of cancer.

CT (computed tomography): Joints with usual X-ray machinery with computer handing out to produce a sequence of cross sectional shapes of the body that combine to produce a 3-D structures. X-ray Fig. later. CT Fig. s are further described than simple radiographs and provide doctors the capability to see the structures through out the body than different angles. [11]

Fluoroscopy: X-rays or a fluorescent panel to find out real-time Fig. s of motion throughout the object, for example to follow the way of inject or ingest contrast agent. Such as, fluoroscopy is responsible to observe the motion of the heart beat, and with the help of radiographic compare agent, to see the blood stream to the heart muscles and as by blood vessels and organs. This expertise is responsible by a radiographic contrast representative to show the internal thread catheter throughout cardiac angioplasty, which is a simply invasive procedure to open the blocked arteries which provide blood towards heart. [30]

Therapeutic

X-rays and some another kinds of highly-powerful radiation should be reasponsible to demolish cancerous lumps and cells by destroying their DNA. The dosage responsible for the treatment of cancer which is high as compare to the radiation dosage responsible for find out the images. It comes by a machine outer surface of the body which is located within the body, within or near lump cells, or injected into the blood flow. [30].

Are there risks?

The diagnostic responsible of X-ray scan considerably compensate the risk. X-ray scans identify probably life-threatening ways such as clogged blood vessel, bone cancer, and infection. On the other hand X-rays forms ionizing radiation–a type of radiation which is responsible to damage living tissue potentially. It increases by exposure added up over the life of the person. The threat of increasing cancer by radiation coverage is small. [28]

An X-ray in an expecting woman creates no recognized risk to the infant if the part of the area being Fig. d isn't the tummy or pelvis. Generally, if imaging of the tummy and pelvis is needed, doctors desire to utilize exams that don't utilize radiation, for example MRI or ultrasound. Anyhow, If no one can provide the answer required, an X-ray probably a suitable alternative imaging choice.

Children be extra responsive to ionizing radiation having a lengthy life expectation and, therefore, a maximum relative threat for emergent cancer as compare to adults. Parents request the technologist if their machine setting has been accustomed for children.

"What are NIBIB-funded researchers developing in the field of X-ray technology?" [29]

Present investigations of X-ray expertise focus on the procedures to decrease radiation dosage, get better shape resolution, and improve difference materials and procedures.

Dedicated Breast CT: Investigation funds by NIBIB has lead to the formation of a breast CT scanner (bCT) that permits the technologist to observe the breast in 3-D and have ability to expose tiny lumps hidden at the back of hard breast muscles. It is responsible a radiation dosage than mammography by transfer X-rays only by the breast and not the upper body. Now a day, over 600 women contain various shapes by using bCT in clinical trial. Outcomes from this trial propose that bCT is considerably good at diagnosing lumps than mammography, it is improved to detect microcalcifications. In recent times, position emission tomography (PET) technologies have been included into the bCT area. A PET scan thing to see areas of improved metabolic action, which might point to the occurrence of a lump. Furthermore, injection of a difference agent have been exposed to get better bCT's capability to identify

microcalcifications and assist to radiologists differentiate benevolent from malignant lumps. Research is now a day pay attention on procedures in which bCT might be responsible to give real-time Fig. control for biopsy needle placement and simply persistent ablation of lumps. [29]

*Near-infrared, Diffuse Light Imaging with Ultrasonic control***:** Investigators funded by NIBIB have oraganized a new, hand-held breast imaging technology which is responsible visible glow to differentiate benign cuts from initial-stage cancer. The systems create maps of muscles density in a confined area of the breast based on about the muscles is cancerous. The way is now to be checked in a huge number of objects undergoes surgery to eliminate a breast lump. Initial results shows that the imaging system might be a promising adjunct to mammography for identification of breast cancer and finding disease prognosis. As well, the structure could permit surgeons to extra quickly to findout the lump margins during surgery compare to procedures used over the past twenty years. This might potentially decrease surgeries that required to be repetition due to not all cancerous muscles but was eliminated at first.

Now-a-days almost all hospitals, diagnostic centers have equipments which use X-rays for identification and treatments.

A lot of information on application of radiation in medicine is available in chapter 9 (Radiation used for diagnostic purpose in the book, [30] "Radiation and Health by Themod Henriksen and Biophysics Group, University of Oslo (2013).

Highlights for X-ray diagnostic

Ref. Thermod Henriksen and his Biophysic Groups' book [30]. They have first mentioned the developments in a chronological order.

1900 – Chest X-ray helped detection of TB and treatment.

1906-1912 – X-ray contrast medium was introduced in diagnostic radiotherapy. If two organs have similar densities and similar average atomic numbers, it is not possible to distinguish them on a radiograph, because no natural contrast exists. Consequently contrast compounds, like iodine compounds, Barium sulphate are used.

1913 – The most important invention (to help generate X-rays for radiology) was made by William Coolidge in 1913 when he made Coolidge X-ray tube. It was a very good product and gave brilliant X-ray source.

1929 – Cardiac characterization was first performed by Werner Forssmann with the help of contrast compounds – a catheter was advanced from a vein in the arm into the right atrium of the heart. For this remarkable achievement, Forssmann won Nobel Prize in 1956.

1955 – The X-ray image intensifier was developed. It allowed the pickup and display of the X-ray movie using a T.V. camera and monitor, further improved with the use of an image intensifier/TV combination, leading to angiography technology.

1970 – X-ray mammography was developed for checking cancer in breasts, a very big steps in preventive medicine.

1972 – Computed Tomography (CT) was developed by Godfrey Hounsfield and Allan Cormack. They won the Nobel Prize in 1979.

But in 1948 Marius Kolsrud of Oslo University had made an equipment to take X-ray pictures of a single plane in the object. The X-ray source and the film moved in opposite directions. This technique was extremely useful to scan the lungs in connection with tuberculosis.

1976 – Andreas Gruentzig, a surgeon in the University Hospital Zurich, Switzerland, invented coronary angioplasty by using X-ray fluoroscope.

1984 – Three dimensional image processing using digital computers and CT or MR data. 3-dimensional images of bones and organs were first made.

Physical basis for X-ray picture

The X-ray picture of the part of the body that is between the X-ray tube and the film. Only the X-ray protons that penetrate the object and reach the film can give a signal or blackening of film. You cannot see the photons that are absorbed or scattered. To see into the body, you must have something that can penetrate the body – come out again – and give information. Fig. 47 illustrates the main points for making an X-ray photo.

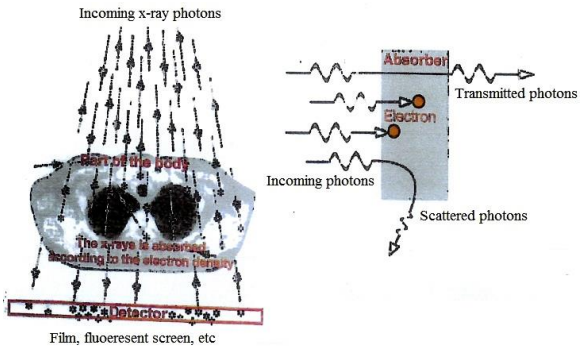

Fig. 47: Two drawings – one vertical and one horizontal –are attempts to illustrate the basic principles of an x-ray photo. Important issues to discuss are: 1. The x-ray source; 2. The absorption and scattering in the body; 3. The detector system. [30].

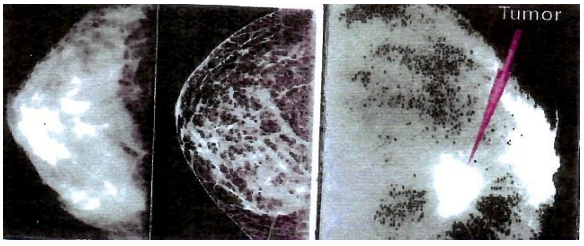

Fig. 48: In the example on the left we see two mammograms of the same normal breast. The large differences are due to the technique used. To the left is a modern digital picture whereas the other is a film-based mammography. [30].The book by Thermod Henriksen *et al.* [30] describes further, in detail, (1) The X-ray source (2) Absorption and scattering in the body (3) Photoelectric effect – variation with photon energy (4) Compton effect – variation with atomic number (4) Compton effect – variation with photon energy (5) Compton effect – variation with atomic number (3) The detector system (4) Mammography (Fig. 48) (5) Implants (6) Fluoroscopy (6) Digital imaging (7) CT – Computer tomography (Fig. 49) (8) Fluoroscopy (Fig. 50) (9) Backscattered X-rays – Compton scattering (Fig. 51) (10) Use of radioactive isotopes (nuclear medicine) – Isotopes used as tracers – isotopes in radiation therapy – isotopes for diagnostic purposes.

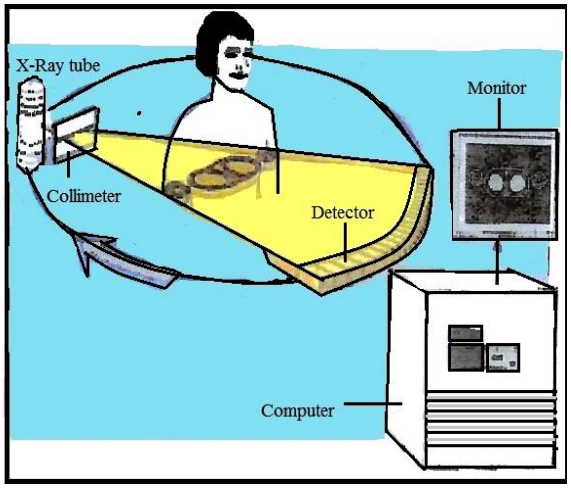

Fig. 49: a The illustration gives some of the same properties of a CT-scanner. [30].

Fig. 49-b ACT-scanner used in hospitals. [30]

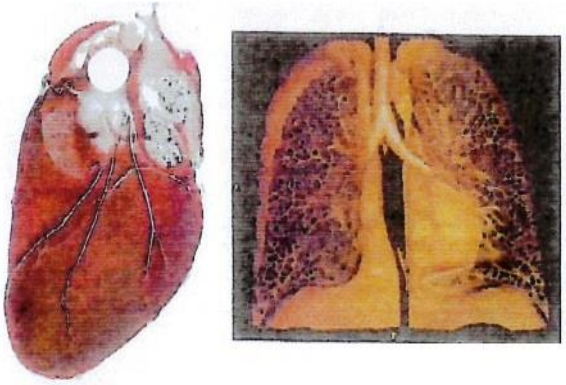

Fig. 50: CT-scan pictures of a heart and lungs. [30]

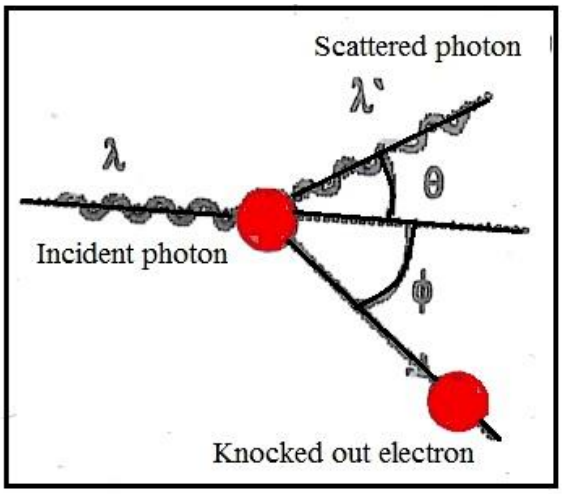

Fig. 51: Backscattered x-rays – Compton scattering. [30].

Since Computer Tomography (CT) and CT-PET (Position Emission Tomography) play very important roles in medical diagnostics, we are taking the liberty to mention the principles of these two techniques.

CT – Computer Tomography

These procedures play a very beneficial role in the treatment of TB in the 1950s and 1960s. The technique is rely on the simple principle of moving synchronously and in opposite directions the X-ray tube and the film. This results in sharper structures in the focal plane. This procedure was planned in the 1900s by the Italian radiologist Alessandro Vallebona and in Norway Professor Marius Kolsrud had construct the first apparatus in 1948. In 1972, Dr. G. N. Hounsfield and Dr. A.M. Cormack introduced, successfully the CT or CAT scanner since much smaller contrast differences could be observed. They replace the X-ray film by a group of small detectors. The signals from the detectors are store and analyze mathematically in a computer. The computers rapidly reconstruct an image of the examine cross-section. Scintillation detectors collective with photomultipliers have been used of late. Fig. 49, 50 give some of the major properties of a CT-scanner.

CT – PET – Positron Tomography

The procedure based on artificially induced isotopes which emits positrons. In the usual β-decay, a neutron is transformed into a proton and an electron, which was emitted (Fig. 52). This favorable reaction since the neutron mass is higher than the proton mass. The opposed reaction where a proton is altered into a neutron is, rather, a more tricky process. The goal can attained by two different routes, viz., (1) Electron capture and (2) positron emission. For all natural isotopes, electron confine is the usual process – because the energy between the parent and daughter is fewer than $2m_ec^2$ (m_e is the electron mass). On the other hand, for a number of artificially induced isotopes positron emission done. The fate of the emitted positron is; after being slowed down, it will meet an electron, and then either annihilate directly, or form a short-lived "positronium atom". The last process is annihilation where the mass of the two particles is altered into γ-ray photons. Mainly two photons with identical energy, 511 KeV, are formed. An important point is that the photons fly off in opposite directions (see the illustration to the right). These annihilation processes represent the basic physical principle of PET. We observed two photons by detectors 180 degrees apart (coincidence measurements). We know from this observation that the annihilation process has taken place somewhere along the line shown in the illustration (52).

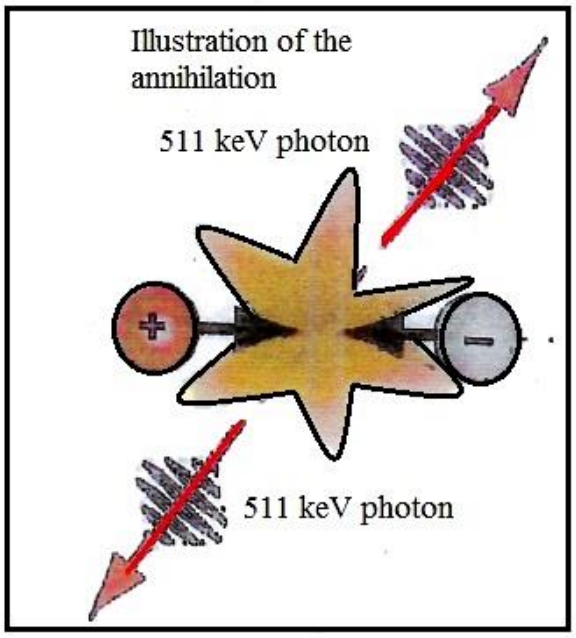

Fig. 52: Positron emission tomography. Illustration of the annihilation of positron with electron. [30].

PET: can find out the position of the radioactivity by chance measurements of photons with energy 511 KeV. One observation yields a line whereas two or more observations in other directions give a point where the radioactivity has its origin. If we in addition have CT or MR measurements for body reference we can find out where in the body we find the radioactivity.

PET can give us:

1. Knowledge on how tissue and organs activity on both the molecular and cell level.
2. PET is significant to examine cancer – and in particular provide information regarding metastases.
3. With PET it is probable to follow the effect of a treatment.
4. It is also possible to study change in the brain that follows Alzheimer disease and epilepsy.

In PET scan you get information on metabolic changes on the cell level. Consequently, PET Fig. 53) can, to a large extent, observe cancer at an early stage – when the changes are on the cellular level. For CTS and MRI malign changes can only be observed when the structure of the organs and the tissues is changed.

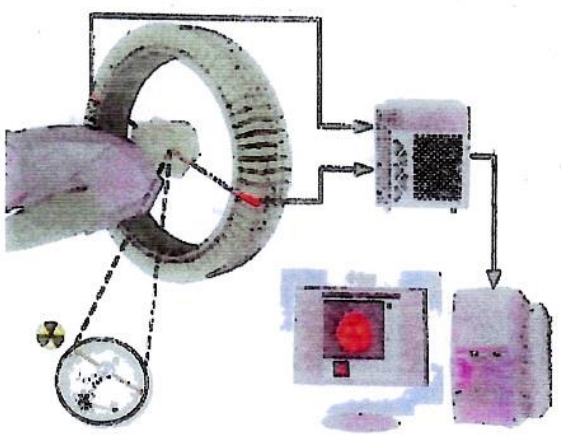

Fig. 53: An illustration with a good introduction to PET. The detectors are placed in a ring around the patient. Coinsidences for two opposite detectors are measured and a picture is reconstructed. For reference with the body, CT or MR is used. [30].

Professor Aadne Ore of the University of Oslo described PET in these words:

"The atom is a submicroscopic double star. The two partners, the electron and the positron are in a brief dance of death, which ends with material annihilation and a flare of electromagnetic radiation. The flare is the origin of PET".

Practical tips for a better characterization of materials through X-ray diffraction (XRD)

Instruments used for X-ray diffraction

"We know that the process of X-ray production results from bombarding a metallic target with electrons. The electrons, accelerated by an electric field, are suddenly slowed down when they hit the target and lose some of their energy, which is dispersed in the form of radiation, a process called braking radiation (Bremsstrahlung in German). The resulting X-rays do not have a specific wavelength, the emission spectrum is continuous and its intensity increases with the electron acceleration voltage." [20] René Guinebretière [20] of the Ecole Nationale Superiéure de Céramiques Industrielles, Limoges, France, in his book "X-ray Diffraction by Polycrystalline Materials| by ISTE, UK (2007), dedicated a whole chapter to this topic. Most of the books on X-ray diffraction contain this information, but not as a packet. The other most important and useful source on all aspects of X-ray diffraction is from Dr. Scott A. Speakman of the Massachusettes Institute of Technology, USA – Ref. http://prism.mit.edu/xray. We are using both these sources in this section.

The book by Réne Guinebretière has dealt with almost all of the instruments.

Instrumentation used for X-ray diffraction [20]

The different elements of a diffractometer
X-ray sources
Crookes tubes
Coolidge tubes
High intensity tubes
Synchrotron radiation

Filters and monochromator crystals

Filters
Monochromator crystals
Multi-layered monochromators or mirrors

Detectors

Photographic film
Gas detectors
Solid detectors

Diffractometers designed for the study of powdered or bulk polycrystalline samples
The Debye-Scherrer and Hull diffractometer
The traditional Debye-Scherrer and Hull

The modern Debye-Scherrer and Hull diffractometer: use of position sensitive detectors
Focusing diffractometers: Seeman and Bohlin diffractometers
Principle
The different configurations
Bragg-Brentano diffractometers
Principle
Description of the diffractometer; path of the X-ray beams
Parallel geometry diffractiometers
Diffractometers equipped with plane detectors

Diffractometers designed for the study of thin films

Fundamental issue
Introduction
Penetration depth and diffracted intensity.
Conventional diffractometers designed for the study of polycrystalline films ..
Systems designed for the study of textured layers
High resolution diffractometers designed for the study of epitaxial films
Sample holder

An introduction to surface diffractometry

Many useful photographs of instruments used in the application of X-ray diffraction are available in the books of Prof.Dr. René Guinebretiere [20], Prof.Dr. B.D. Cullity [11] and Prof.Dr. Lesley E. Smart & Prof.Dr. Elaine A. Moore [31].

Acknowledgements

We are extremely grateful and indebted to all the authors, especially Prof. Dr. René Guinebretière, Prof.Dr. B.D. Cullity, Prof. Dr. S.R. Stock, Prof. Dr. A Guinier, Prof. Dr. R.E. Reed-Hill, Prof. Dr. S.K. Chatterjee, etc, etc, and to the publishers of their invaluable works for quoting their works in detail, with proper references. The use of this literature is exclusively for the dissemination of X-ray diffraction techniques and their uses for students of materials science, chemistry, solid state physics, etc. No financial or commercial interest whatsoever is involved.

References

1. O. Glasser, Wilhelm Conrad Röntgen and the Early History of the Röntgen Rays, John Bale Sons and Daniels Son Ltd., London (1933).
2. w. f. Smith, Principles of Material Science and Engineering, 2nd Ed., McGraw-Hill International Editions, Engineering Series, USA (1990).
3. W. C. Röntgen, in Willaim Conrad Röntgen, Dictionary of Scientific Biography, Scribner's, New York (1975).
4. G. L. Clark, Applied X-rays, McGraw Hill, New York (1953).
5. H. Klug, and L. Alexander, X-ray Diffraction Procedures, John Wiley & Sons, New York (1954).
6. F. Bueche, Principles of Physics, 4th Edition, McGraw International Book Co., London, USA (1984).
7. R. E. Reed-Hill, Physical Metallurgy Principles, D. Van Nostrand Company, USA (1973).
8. G. Thomas, Transmission Electron Microscopy of Metals, John Wiley & Sons, USA (1981).
9. (A) Introduction to Powder/Polycrystalline Diffractions – Basics of X-ray Diffraction, Thermo ARL, ARL Applied Research Laboratories S.A. Publications, Switzerland (1999). (B) X-ray Diffraction (XRD), http://www.matter.org.uk/diffraction/x-ray/default.html.
10. (A) X-ray Christallography, Libre Texts – Chemistry, CCBY-NC-SA 30 US, 9.7.2018. (B). Sands, D.E., Introduction to Crystallography, Dover Publications, Inc., New York (1975). (C) Giacovazzo, C., Fundamentals of Crystallography, Oxford University Press, Oxford, U.K. (1992).
11. (A). Cullity, B.D., Elements of X-ray Diffraction (2nd Ed.), Addison Wesley Publications Co., Reading, Mass. USA (1978). (B) Cullity, B.D. and S.R. Stock, Pearson India, Noida, UP-201309, India (2015).
12. H. P. Klug, and L. E. Alexander, X-ray Diffraction Procedures, 2nd Ed, J. Wiley and Sons, New York (1974).
13. B. E. Warren, X-ray Diffraction, Addison-Wesley, Reading, Mass. (1990).
14. B. E. Warren, and B.L. Averbach, The Effect of Cold Work Distortion on X-ray Patterns, *J. Appl. Physics*, **21,** 23 (1952).
15. M. S. Paterson, X-ray Diffraction by Face-Centred Cubic Crystals with Deformation Faults, *British J. Appl. Physics*, 23 (1952).
16. M. S. Paterson, X-ray Diffraction and the Density of Faults, Report Research School of Earth Sciences, Inst. Of Adv. Studies, Australian National University, Canberra, ACT 2601, Australia (6.7.1988).
17. J. M. Robertson, X-ray Analysis and Application of Fourier Series Procedures to Molecular Structure, Progress in Physics **4**, (1937).
18. I. N. Snedden, Fourier Transforms, McGraw-Hill Book Co., Inc., New York (1951).
19. A. Guinier, X-ray Diffraction in Crystals, Imperfect Crystals and Amorphous Bodies, Dover Publications, New York (1994).
20. Guinebretière, René, X-ray Diffraction by Polycrystalline Materials, ISTE Ltd., London (2007).
21. E. C. Titmarsch, Theory of Fourier Integrals, Clarendon Press, Oxford (1937).
22. W. Clegg, Crystal Structure Determination, Oxford University Press, Oxford (1998).
23. H. Lipton, and W. Cochran, Determination of Crystal Structure, G. Bell & Sons, London (1953).
24. S. K. Chatterjee, X-ray Diffraction – Its Theory and Applications, PHI Learning Pvt. Ltd., New Delhi (2010).
25. W. Massa, Crystal Structure Determination, Springer Verlag, Berlin (2004).
26. R. L. Garrod and G.A. Hawkes, X-ray Stress Analysis of Plastically Deformed Metals, *British J. App. Phy.*, **4**, 7 (1963).
27. L. G. Schulz, Procedure of Determining Favoured Orientation of a Flat Reflection Sample Using a Geiger Counter X-ray Spectrometer, *J. App. Phy*, **20**, 1030 (1949).
28. History of Radiography - NDT Resource Centre, https://www.nde-ed.org/EducationCommunity College/Radiography/Introduction/history,htm (9.11.2018).
29. X-rays, National Institute of Biomedical Imaging and Bio-engineering, USA (Oct. 2017).

30. Application of Radiation in Medicine in Radiation and Health, Thormod Hendriksen and Biophysics Group, University of Oslo, Chapter 9 (2013). https://www.mn.uio.no/fysikk/english/services/knowledge/radiation-and-health/chap09

31. Smart, E. Lesley, and Elaine A. Moore, Solid State Chemistry – An Introduction, 4th Edition, CRC Press (Tailor & Francis Group) USA (2012).